Supplementary Information for

# An $S = ½$ iron complex featuring $N_2$, thiolate, and hydride ligands: Reductive elimination of $H_2$ and relevant thermochemical Fe-H parameters.

Nina X. Gu, Paul H. Oyala and Jonas C. Peters*

Division of Chemistry and Chemical Engineering
California Institute of Technology
Pasadena, California 91125, United States

*Email: jpeters@caltech.edu

*General considerations.* All syntheses and measurements, unless otherwise stated, were carried out under an inert atmosphere ($N_2$) in a glovebox or using standard Schlenk techniques, and solvents were dried and degassed by thoroughly sparging with $N_2$ and then passing through an activated alumina column in a solvent purification system supplied by SG Water, LLC. Deuterated solvents were purchased from Cambridge Isotope Laboratories, Inc., degassed, and dried over activated 3 Å molecular sieves before use. 2-phenylbenzenethiol,[1] bis(*o*-diisopropylphosphino-phenyl)-chlorosilane (**4**),[2] lithium triethylborodeuteride[3] were prepared according to literature procedures. All other reagents were purchased from commercial vendors and used without further purification unless otherwise stated.

*Physical methods.* Electrochemical measurements were carried out in a glovebox under an $N_2$ atmosphere in a one compartment cell using a CH Instruments 600B electrochemical analyzer. A glassy carbon electrode was used as the working electrode and a platinum wire was used as the auxiliary electrode. A silver pseudoreference electrode was used with the ferrocene couple ($Fc/Fc^+$) as an internal reference, unless otherwise noted. Solutions of electrolyte (0.4 M $[NBu_4][PF_6]$ in THF) and analyte were also prepared under an $N_2$ atmosphere. NMR spectra ($^1H$, $^{13}C$, $^{31}P$) were collected on Varian 300, 400, or 500 MHz spectrometers (25 °C unless otherwise specified). $^1H$ and $^{13}C$ chemical shifts are reported in ppm, relative to tetramethylsilane using residual proton and $^{13}C$ resonances from solvent as internal standards. $^{31}P$ chemical shifts are reported in ppm relative to 85% aqueous $H_3PO_4$. Thin film IR spectra were obtained using a Bruker Alpha Platinum ATR spectrometer with OPUS software in a glovebox under an $N_2$ atmosphere. Optical spectroscopy measurements were taken on a Cary 50 UV−Vis spectrophotometer using a 1-cm quartz cell, unless otherwise noted. Temperature regulation for UV-Vis measurements was carried out with a Unisoku cryostat. Time-course UV-Vis spectra were collected with the Scanning Kinetics application of the Cary WinUV software and fit to Gaussian lineshapes with the Curve Fitting tool of Matlab. $H_2$ was analyzed on an Agilent 7890A gas chromatograph (HP-PLOT U, 30 m, 0.32 mm ID; 30 °C isothermal; nitrogen carrier gas) using a thermal conductivity detector. Combustion analyses were carried out by either Midwest Microlabs (Indianapolis) or the Beckman Institute Crystallography Facility (Caltech).

*X-ray crystallography.* X-ray diffraction measurements were carried out in the Beckman Institute Crystallography Facility. XRD measurements were collected using a dual source Bruker D8 Venture, four-circle diffractometer with a PHOTON CMOS detector. Structures were solved using SHELXT and refined against $F^2$ on all data by full-matrix least squares with SHELXL. The crystals were mounted on a glass fiber under Paratone N oil.

*DFT calculations.* Optimization and frequency calculations were performed using the Gaussian 09 program.[4] Structures of **8-H** and **9** were optimized using the crystal structure coordinates as the input. Structures utilized for thermochemical estimations were optimized with MeCN solvation. The M06-L functional[5] with the def2-TZVP[6] basis set was used on Fe, and the def2-SVP basis set was used on all other atoms. DFT-estimated free energies of of $H^-$ transfer in MeCN are referenced to $H^-$ dissociation from TEMPO in MeCN (BDFE of TEMPO-H = 66.5 kcal/mol).[7]

*$^{57}$Fe Mössbauer spectroscopy.* Mössbauer spectra were recorded on a spectrometer from SEE Co. (Edina, MN) operating in the constant acceleration mode in a transmission geometry. The sample was kept in an SVT-400 cryostat from Janis (Wilmington, MA). The quoted isomer shifts are

relative to the centroid of the spectrum of a metallic foil of α-Fe at room temperature. Solid samples were prepared by grinding polycrystalline material into a fine powder and then mounted in a Delrin cup fitted with a screwcap as a boron nitride pellet. Frozen solution samples were prepared by freezing the sample in a Delrin cup. All samples were prepared within a glovebox with rapid transfer to a liquid nitrogen bath before mounting in the cryostat. Data analysis was performed using the program WMOSS (www.wmoss.org) and quadrupole doublets were fit to Lorentzian lineshapes.

*CW EPR spectroscopy.* 77 K X-band EPR spectra were obtained on a Bruker EMX spectrometer on solutions prepared as frozen glasses in 2-MeTHF. Spectra were simulated using the EasySpin[8] suite of programs with Matlab.

*Pulse EPR spectroscopy.* All pulse Q-band (≈ 33.7 GHz) EPR and electron nuclear double resonance (ENDOR) experiments were aquired using a Bruker (Billerica, MA) ELEXSYS E580 pulse EPR spectrometer equipped with a Bruker D2 resonator. Temperature control was achieved using an ER 4118HV-CF5-L Flexline Cryogen-Free VT cryostat manufactured by ColdEdge (Allentown, PA) equipped with an Oxford Instruments Mercury ITC.

Pulse Q-band ENDOR was acquired using the Davies pulse sequence ($\pi - T_{RF} - \pi_{RF} - T_{RF} - \pi/2 - \tau - \pi -$ echo), where $T_{RF}$ is the delay between mw pulses and RF pulses, $\pi_{RF}$ is the length of the RF pulse and the RF frequency is randomly sampled during each pulse sequence.

In general, the ENDOR spectrum for a given nucleus with spin $I$= ½ ($^1$H, $^{31}$P) coupled to the S = ½ electron spin exhibits a doublet at frequencies

$$\nu_{\pm} = \left|\frac{A}{2} \pm \nu_N\right| \tag{1}$$

Where $\nu_N$ is the nuclear Larmor frequency and $A$ is the hyperfine coupling. For nuclei with $I \geq 1$ ($^2$H), an additonal splitting of the $\nu_{\pm}$ manifolds is produced by the nuclear quadrupole interaction (P)

$$\nu_{\pm,m_I} = \left|\nu_N \pm \frac{3P(2m_I - 1)}{2}\right| \tag{2}$$

Simulations of all pulse EPR data were achieved using the EasySpin[8] simulation toolbox (release 5.1.8) with Matlab 2016 using the following Hamiltonian:

$$\hat{H} = \mu_B \vec{B}_0 g \hat{S} + \mu_N g_N \vec{B}_0 \hat{I} + h\hat{S} \cdot \boldsymbol{A} \cdot \hat{I} + h\hat{I} \cdot \boldsymbol{P} \cdot \hat{I} \tag{3}$$

In this expression, the first term corresponds to the electron Zeeman interaction term where $\mu_B$ is the Bohr magneton, g is the electron spin g-value matrix with principle components g = [$g_{xx}$ $g_{yy}$ $g_{zz}$], and $\hat{S}$ is the electron spin operator; the second term corresponds to the nuclear Zeeman interaction term where $\mu_N$ is the nuclear magneton, $g_N$ is the characteristic nuclear g-value for each nucleus (e.g. $^1$H,$^2$H,$^{31}$P) and $\hat{I}$ is the nuclear spin operator; the third term corresponds to the electron-nuclear hyperfine term, where $\boldsymbol{A}$ is the hyperfine coupling tensor with principle components $\boldsymbol{A}$ = [$A_{xx}$ $A_{yy}$ $A_{zz}$]; and for nuclei with $I \geq 1$, the final term corresponds to the nuclear

quadrupole (NQI) term which arises from the interaction of the nuclear quadrupole moment with the local electric field gradient (efg) at the nucleus, where $\boldsymbol{P}$ is the quadrupole coupling tensor. In the principle axis system (PAS), $\boldsymbol{P}$ is traceless and parametrized by the quadrupole coupling constant $e^2Qq/h$ and the asymmetry parameter $\eta$ such that:

$$\boldsymbol{P} = \begin{pmatrix} P_{xx} & 0 & 0 \\ 0 & P_{yy} & 0 \\ 0 & 0 & P_{zz} \end{pmatrix} = \frac{e^2Qq/h}{4I(2I-1)} \begin{pmatrix} -(1-\eta) & 0 & 0 \\ 0 & -(1+\eta) & 0 \\ 0 & 0 & 2 \end{pmatrix} \qquad (4)$$

where $\frac{e^2Qq}{h} = 2I(2I-1)P_{zz}$ and $\eta = \frac{P_{xx}-P_{yy}}{P_{zz}}$. The asymmetry parameter may have values between 0 and 1, with 0 corresponding to an electric field gradient with axial symmetry and 1 corresponding to a fully rhombic efg.

The orientations between the hyperfine and NQI tensor principle axis systems and the g-matrix reference frame are defined by the Euler angles (α, β, γ).

*Synthesis and characterization of compounds **2** – **11***

**2-(isopropylthio)biphenyl (2)**
A mixture of 2-phenylbenzenethiol (26.5 g, 0.142 mol), 2-bromopropane (17.5 g, 0.142 mol) and $K_2CO_3$ (29.4 g, 0.213 mol) in acetone (500 mL) was allowed to reflux for 5 h. The reaction was cooled to room temperature and filtered through Celite. The filtrate was concentrated to an oil and purified *via* vacuum distillation to yield the title compound as a pale yellow oil (26.0 g, 80 %). $^1$H NMR ($CDCl_3$, 400 MHz, 298 K, δ): 7.49-7.22 (m, 9H), 3.20 (hept, *J* = 6.7 Hz, 1H), 1.19 (d, *J* = 6.9 Hz, 6H). $^{13}$C NMR ($CDCl_3$, 101 MHz, 298 K) δ 143.5 (s), 141.1 (s), 134.7 (s), 130.7 (s), 130.5 (s), 129.6 (s), 127.9 (s), 127.7 (s), 127.3 (s), 126.1 (s), 37.3 (s), 23.0 (s).

**(2-(isopropylthio)-[1,1'-biphenyl]-3-yl)lithium · 0.5 TMEDA (3)**
Neat tetramethylethylenediamine (4.0 mL, 26.7 mmol) and *n*-BuLi (16.4 mL, 1.6 M in hexanes) were sequentially added dropwise to a stirring solution of compound **2** (6.0 g, 26.3 mmol) in pentane (100 mL) at 0 °C. The yellow reaction mixture was stirred at 23 °C overnight, which yielded ample white precipitate. The solids were collected by filtration and washed with pentane (3 x 10 mL) to yield the title compound as an off-white solid. (6.75 g, 88%) $^1$H NMR ($C_6D_6$, 400 MHz, 298 K, δ): 8.05 (bs, 1H), 7.79 (d, *J* = 6.0 Hz, 2H), 7.41-7.31 (m, 3H), 7.21-7.17 (m, 2H), 2.98 (bs, 1H), 1.91 (s, 6H, TMEDA), 1.75 (s, 2H, TMEDA), 1.06 (bs, 6H).

**$HSiP_2S$ (5)**
A suspension of compound **3** (4.54 g, 15.5 mmol) in toluene (20 mL) was added to a stirring solution of bis(*o*-diisopropylphosphino-phenyl)-chlorosilane (**4**) (5.84 g, 12.9 mmol) in toluene (30 mL) at –78 °C. The reaction mixture was stirred for 12 h, with gradual warming from –78 °C to 23 °C. The resulting orange reaction mixture was filtered through Celite and concentrated. The resulting orange oil was triturated with pentane (20 mL) to yield the title compound as an off-white solid, which was isolated by filtration and washed with cold pentane (–78 °C, 40 mL). The filtrate was concentrated to 10 mL and stored at –33 °C overnight, which yielded additional product. (5.47 g, 66 %) $^1$H NMR ($C_6D_6$, 400 MHz, 298 K, δ): 7.55 (d, *J* = 7.3 Hz, 2H), 7.44 (d, *J* = 8.0 Hz, 2H),

7.40 (d, $J$ = 7.5 Hz, 2H), 7.29-7.26 (m, 3H), 7.23-7.16 (m, 3H), 7.11-7.01 (m, 4H), 2.99 (hept, $J$ = 6.3 Hz, 1H), 2.14-1.98 (m, 4H), 1.15 (m, 12H), 1.04-0.97 (m, 18H). $^{31}$P NMR ($C_6D_6$, 162 MHz, 298 K, δ): 1.10 (s). IR (solid, cm$^{-1}$): 2228 (Si-H). ESI-MS (positive ion, amu): Calcd. 643.3 ([M+H]$^+$); Found. 643.2.

**[(SiP$_2$S)Fe]$_2$(μ-N$_2$) (6)**

A solution of **5** (1.0 g, 1.6 mmol) in THF (15 mL) was added to solid $FeCl_2$ (0.28 g, 1.6 mmol) and stirred for 9 h. The reaction mixture was cooled to -78 °C, and MeMgCl (3.0 M in THF, 1.6 mL) was added dropwise to the stirring solution. The reaction mixture was stirred overnight with gradual warming from –78 °C to 23 °C and stirred at 23 °C for an additional day. The reaction mixture was filtered through Celite and concentrated to dryness. The resulting brown solids were washed with pentane (20 mL), extracted with $C_6H_6$ (50 mL) and lyophilized. The brown material was redissolved in $C_6H_6$ (20 mL) and filtered through Celite. The filtrate was lyophilized to yield the title compound as a dark brown solid. (crude yield: 1.09 g, 52%) Smaller portions of the crude product were recrystallized prior to use: Pentane (10 mL) was layered over a benzene (5 mL) solution of **4** (160.0 mg, 0.1 mmol) and allowed to stand at 23 °C, which yielded the product as dark brown blocks (62.4 mg, 39% yield from recrystallization). Dark brown crystals suitable for XRD were grown from slow evaporation of a $Et_2O$ solution at 23 °C. $^1$H NMR ($C_6D_6$, 300 MHz, 298 K, δ): 83.0, 52.6, 27.0, 13.7, 9.9, 8.7, 7.2, 6.4, 6.0, 4.9, 4.0, 3.6, 3.3, -2.5, -7.7, -70.3. $\mu_{eff}$ ($C_6D_5CD_3$, Evans method, 298 K): 4.8$\mu_B$. IR (solid, cm$^{-1}$): 1888 (N≡N). UV-Visible (THF, 298 K, nm {M$^{-1}$cm$^{-1}$}): 495 {4478}, 678 {1273}, 773 {1250}, 1019 {1210}. Anal. Calcd. for [(SiP$_2$S)Fe]$_2$(N$_2$)·(C$_6$H$_6$)$_{0.5}$ ($C_{75}H_{141}Fe_2N_2P_4S_2Si_2$): C, 65.45; H, 6.66; N, 2.04. Found: C, 65.51; H, 7.03; N, 2.16.

**[(SiP$_2$S)Fe(H)(N$_2$)]Li(THF)$_2$ (7-H)**

To a stirring solution of **6** (0.100 g, 0.074 mmol) in THF (5 mL), $LiEt_3BH$ (1.0 M in THF, 0.16 mL) was added dropwise at –78 °C. The reaction mixture was stirred at 23 °C for 30 min. The reaction mixture was subsequently chilled to –78 °C, and a second portion of $LiEt_3BH$ (1.0 M in THF, 0.16 mL) was added. The dark red reaction mixture was stirred at 23 °C for 30 min, and the volatiles were then removed *in vacuo*. The resulting red residue was washed with 2:1 pentane/$Et_2O$ (3 mL) and pentane (10 mL) then extracted with THF (10 mL) to yield compound **7-H** as a red solid. (97.3 mg, 78%) Dark red crystals suitable for XRD were grown from slow evaporation of a $Et_2O$ solution into HMDSO at 23 °C. $^1$H NMR ($C_6D_6$, 400 MHz, 298 K, δ): 8.58 (d, $J$ = 7.4 Hz, 2H), 8.10 (d, $J$ = 7.4 Hz, 1H), 7.71 (d, $J$ = 7.5 Hz, 2H), 7.52 (d, $J$ = 7.3 Hz, 2H), 7.39 (t, $J$ = 7.3 Hz, 2H), 7.22 (t, $J$ = 7.4 Hz, 2H), 7.10 (t, $J$ = 7.6 Hz, 2H), 6.97 (q, $J$ = 10.3, 9.0 Hz, 2H), 6.88 (d, $J$ = 7.2 Hz, 1H), 3.30 (bs, 8H, THF), 2.78 (bs, 2H), 2.51 (bs, 2H), 1.64 (q, $J$ = 6.9 Hz, 8H, THF), 1.36-1.28 (m, 12H), 1.10-1.00 (m 12H), -19.32 (t, $J$ = 71.3 Hz, 1H). $^{31}$P NMR ($C_6D_6$, 162 MHz, 298 K, δ): 96.8 (s), 96.4 (s). IR (solid, cm$^{-1}$): 2020 (N≡N), 1976 (N≡N), 1935 (N≡N), 1864 (Fe-H); the inequivalent $N_2$ stretches arise from distinct coordination modes of the Li cation. UV-Visible (THF, 298 K, nm {M$^{-1}$cm$^{-1}$}): 336 {6903}, 379 {4263}, 437 {3194}, 535 {1471}. Anal. Calcd. for $C_{44}H_{61}FeLiN_2O_2P_2SSi$: C, 63.30; H, 7.37; N, 3.36. Found: C, 63.32; H, 7.59; N, 3.23.

**[(SiP$_2$S)Fe(D)(N$_2$)]Li(THF)$_2$ (7-D)**

Prepared in an analogous fashion to **7-H** but employing $LiEt_3BD$ (1.0 M in THF). Except for the absence of the hydridic proton resonance at -19.32 ppm, spectroscopic features in the $^1$H NMR spectrum of **7-D** were identical to that of **7-H**. $^{31}$P NMR ($C_6D_6$, 162 MHz, 298 K, δ): 96.85 (t, $J$ =

9.3 Hz). $^{31}P\{^{2}H\}$ NMR ($C_6D_6$, 162 MHz, 298 K, δ): 96.85 (s). IR (solid, $cm^{-1}$): 2016 (N≡N), 1975 (N≡N), 1924 (N≡N); the inequivalent $N_2$ stretches arise from distinct coordination modes of the Li cation.

**[(SiP$_2$S)Fe(H)(N$_2$)][Li(12-crown-4)(THF)] (7-H(crown))**

Neat 12-crown-4 (5.8 µL, 36 µmol) was added in one portion to a homogeneous stirring solution of **7-H** (30 mg, 36 µmol) in $Et_2O$ (10 mL) at 23 °C. Red solids immediately precipitated from solution upon addition of 12-crown-4. The reaction mixture was stirred at 23 °C for 5 min. The resulting solids were isolated by filtration, washed with $Et_2O$ (5 mL) and pentane (5 mL), then extracted with THF (5 mL) to yield the title compound as a red solid. (25.7 mg, 76%) Dark red crystals suitable for XRD were grown from slow diffusion of pentane into a concentrated THF solution at 23 °C. $^{1}H$ NMR (THF-$d_8$, 400 MHz, 298 K, δ): 8.25 (d, $J$ = 6.9 Hz, 2H), 7.60 (d, $J$ = 7.5 Hz, 2H), 7.36 (bs, 3H), 7.19-7.11 (m, 4H), 7.01 (t, $J$ = 7.2 Hz, 3H), 3.62 (bs, 16H, 12-crown-4), 2.60 (bs, 2H), 2.40 (bs, 2H), 1.41 (q, $J$ = 6.8 Hz, 6H), 1.32 (q, $J$ = 6.9 Hz, 6H), 0.78 (q, $J$ = 6.3 Hz, 6H), 0.71 (q, $J$ = 6.4 Hz, 6H), -19.39 (t, $J$ = 69.6 Hz, 1H). $^{31}P$ NMR (THF-$d_8$, 162 MHz, 298 K, δ): 101.20 (s), 100.87 (s). IR (solid, $cm^{-1}$): 1971 (N≡N), 1886 (Fe-H). UV-Visible (THF, 298 K, nm $\{M^{-1}cm^{-1}\}$): 333 {8713}, 421 {4674}, 532 {1906}, 885 {280}. Anal. Calcd. for $C_{48}H_{69}FeLiN_2O_5P_2SSi$: C, 61.40; H, 7.41; N, 2.98. Found: C, 61.26; H, 7.71; N, 2.67.

**(SiP$_2$S)Fe(H)(N$_2$) (8-H)**

*Spectroscopic characterization of **8-H** was carried out on samples generated in situ via the oxidation **7-H** with either [Cp$_2$Co][PF$_6$] or [Cp*$_2$Fe][PF$_6$]*

EPR and ENDOR spectroscopies: Solid [Cp*$_2$Fe][PF$_6$] (1.4 mg, 3.0 µmol) was added in one portion to a solution of **7-H** (4.8 mg, 5.7 µmol) in 2-MeTHF (0.5 mL, –78 °C). The reaction was allowed stir at –78 °C for 1 h and the resulting dark blue solution was filtered through a pre-chilled pipette filter (pipette/glass fiber) to remove excess [Cp*$_2$Fe][PF$_6$]. The filtered solution was analyzed directly. *Note: 77 K X-band EPR spectra of **7-H** generated via oxidation with [Cp$_2$Co][PF$_6$] and [Cp*$_2$Fe][PF$_6$] were identical, see Figure S41.

*For all other spectroscopies, a typical sample preparation is detailed below.*
Solid [Cp$_2$Co][PF$_6$] (2.2 mg, 6.6 µmol) was added in one portion to a solution of **7-H** (5.0 mg) in THF (0.5 mL, –78 °C). The reaction was allowed stir at –78 °C for 1 h and the resulting dark blue solution was filtered through a pre-chilled pipette filter (pipette/glass fiber) to remove excess [Cp$_2$Co][PF$_6$]. This filtered solution was analyzed via the procedures detailed below.

NMR spectroscopy: Sample preparation was carried out in THF-$d_8$, and the filtered solution was analyzed directly.

IR spectroscopy: The filtered solution was utilized to prepare a thin-film for analysis.

UV-visible spectroscopy: The filtered solution was diluted with pre-chilled THF for analysis. *Note: For temperature-controlled UV-vis experiments, the cuvette was allowed to equilibrate for 10 minutes to the set temperature prior to data collection.

$^{57}$Fe Mössbauer spectroscopy: For increased signal-to-noise, ~1 mL of a more concentrated solution of **7-H** was prepared (~ 45 mM in THF) and frozen for analysis.

X-ray diffraction: The filtered solution was concentrated under reduced pressure while kept cold. The resulting dark blue solids were dissolved in a minimal amount of pre-chilled pentane and filtered through a pre-chilled pipette filter (pipette/glass fiber). Dark blue crystals suitable for XRD were grown from slow evaporation of a pentane solution into HMDSO at –33 °C. (The title compound co-crystallized with crystals of $Cp_2Co$.)

$^1$H NMR (THF-$d_8$, 500 MHz, 195 K, δ): 11.0, 5.8, 5.4, 4.7, 3.6, 1.3, 0.9, -7.5. IR (solid, cm$^{-1}$): 2123 (N≡N), 1852 (Fe-H). UV-Visible (THF, 298 K, nm {M$^{-1}$cm$^{-1}$}): 607 {2830}. *Note: The thermal instability of **8-H** precluded characterization by combustion analysis.

**(SiP$_2$S)Fe(D)(N$_2$) (8-D)**
Prepared *in situ* in an analogous fashion to **8-H** but employing **7-D**. IR (solid, cm$^{-1}$): 2121 (N≡N), 1333 (Fe-D).

**[(SiP$_2$S)Fe(N$_2$)][Na(12-crown-4)$_2$] (9)**
A solution of **6** (50 mg, 0.037 mmol) in THF (2 mL) was added to Na(Hg) (12 mg Na, 0.52 mmol; 2 g Hg) and stirred vigorously for 5 h at 23 °C. The resulting red solution was decanted, and neat 12-crown-4 (24 μL) was added in one portion to the reaction mixture. The reaction was stirred at 23 °C for 1 h and subsequently layered with pentane (2 mL). The mixture was allowed to stand at -33 °C overnight, resulting in the precipitation of dark red solids. The solids were collected by vacuum filtration, washed with $Et_2O$ (2 mL x 2) and pentane (2 mL x 2), then extracted with THF (5 mL) to yield the title compound as a red solid. (61.0 mg, 77 %). Dark red crystals suitable for XRD were grown from slow diffusion of pentane into a concentrated THF solution at 23 °C. $^1$H NMR (THF-$d_8$, 400 MHz, 298 K, δ) 11.6, 8.90, 7.6, 6.6, 6.2, 5.7, 3.6, 0.1, -3.3. $\mu_{eff}$ (THF-$d_8$, Evans method, 298 K): 1.8$\mu_B$. IR (solid, cm$^{-1}$): 1963 (N≡N). UV-Visible (THF, 298 K, nm {M$^{-1}$cm$^{-1}$}): 547 {2020}, 826 {499}. Anal. Calcd. for [(SiP$_2$S)Fe(N$_2$)][Na(12-crown-4)$_2$]·THF$_{0.5}$ ($C_{54}H_{80}FeN_2NaO_{8.5}P_2SSi$): C, 59.28; H, 7.37; N, 2.56. Found: C, 58.98; H, 7.66; N, 2.40.

**[(SiP$_2$S)Fe(N$_2$)][K(THF)$_x$] (10)**
A solution of **6** (30 mg, 0.022 mmol) in THF (5 mL) was stirred with potassium metal (25 mg, 0.64 mmol) at 23 °C for 15 min. The resulting dark brown solution was filtered and concentrated to dryness to yield the title complex as a dark brown solid. (37.3 mg) *Note: The broad signals in the room temperature $^1$H NMR spectrum hindered reliable peak integration. $^1$H NMR (THF-$d_8$, 300 MHz, 298 K, δ) 7.92 (bs), 7.63 (bs), 7.23 (bs), 7.02 (t, $J$ = 7.0, 2.2 Hz), 6.79 (bs), 6.43 (bs), 2.41 (bs), 1.09 (bs), 0.78 (bs). $^{31}$P NMR (THF-$d_8$, 121 MHz, 298 K, δ): 93.6 (bs). IR (solid, cm$^{-1}$): 1805 cm$^{-1}$.

**(SiP$_2$S)Fe(NCMe) (11)**
MeCN (0.5 mL) was added to a solution of **6** (50 mg, 0.037 mmol) in $C_6H_6$ (3 mL) at 23 °C, and the resulting dark red solution was stirred at 23 °C for 15 min. The reaction mixture was concentrated to dryness, and the red solids were washed with pentane (3 mL x 2) and extracted with $C_6H_6$ (5 mL). The volatiles were removed *in vacuo*, and the title complex was isolated as a red solid. (48.1 mg, 92%) Dark red crystals suitable for XRD were grown from slow diffusion of

pentane into a concentrated THF solution 23 °C. $^1$H NMR (400 MHz, $C_6D_6$) δ 96.1, 80.5, 51.3, 15.9, 8.9, 8.5, 7.3, 7.2, 6.1, 5.8, 4.2, 2.4, -1.0, -2.8, -4.1, -43.6. $\mu_{eff}$ ($C_6D_6$, Evans method, 298 K): 2.9$\mu_B$. UV-Visible (THF, 298 K, nm {$M^{-1}cm^{-1}$}): 485 {2405}, 680 {325}, 1029 {639}. Anal. Calcd. for $C_{38}H_{47}FeNP_2SSi$: C, 65.60; H, 6.81; N, 2.01. Found: C, 65.72; H, 6.85; N, 1.91

*Quantification of $H_2$ from the conversion of **8-H** to **6***

A representative sample preparation: A filtered solution of **8-H**, which was generated in situ in THF at -78 °C from **7-H** and [$Cp_2Co$][$PF_6$], (see pg. 6, 800 µL, 35.5 mM) was transferred into a Schlenk tube and sealed. The solution was allowed to stir at 23 °C for a minimum of 2 d. An aliquot of the headspace was sampled and analyzed for $H_2$ by GC. Yield of $H_2$: 99% (± 11%)

*Reaction of **7-H(crown)** with $CO_2$ to form **11***

A J. Young NMR tube containing a solution of **7-H(crown)** (4.9 mg, 5.7µmol) in MeCN-$d_3$ (0.5 mL) was degassed via three freeze-pump-thaw cycles and exposed to 1 atm of $CO_2$ at 23 °C. The red solution of **7-H(crown)** turned a darker red color upon addition of $CO_2$. The tube was rotated at 23 °C for 1 h. $^1$H NMR data collected an hour after $CO_2$ addition reveals full consumption of **7-H(crown)** and generation of **11**. Thin-film IR spectrum of the reaction mixture contains a broad stretch at 1605 $cm^{-1}$, consistent with the formation of $HCO_2^-$.

*NMR spectra*

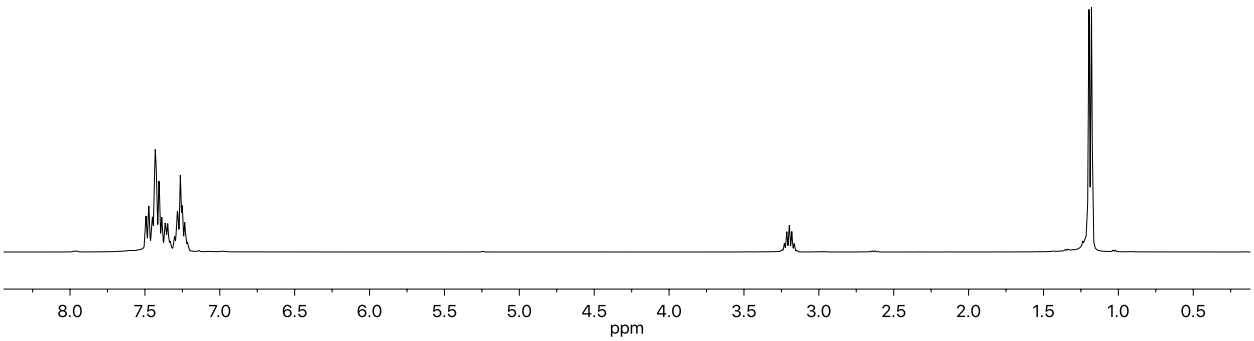


**Figure S1.** $^1$H NMR spectrum (400 MHz) of **2** in $CDCl_3$

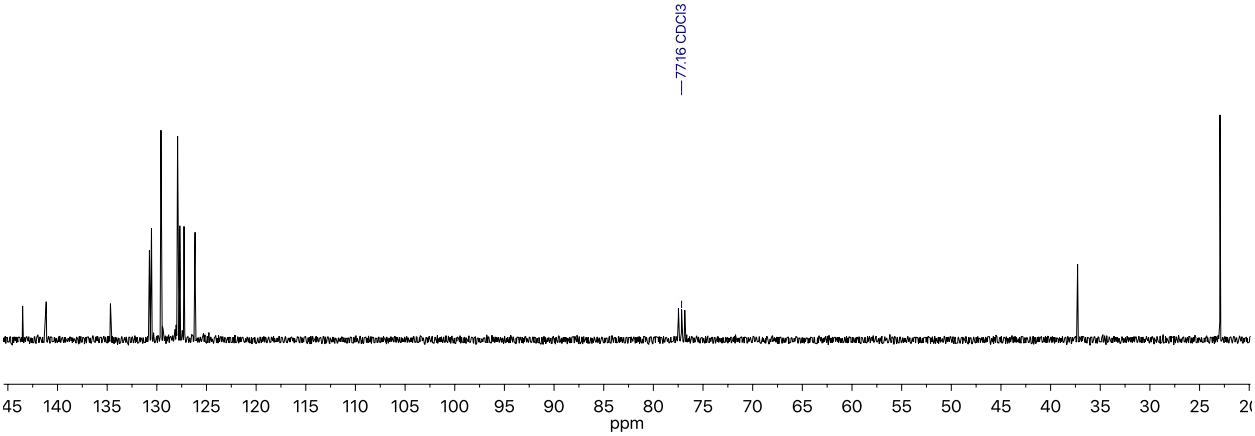


**Figure S2.** $^{13}$C NMR spectrum (101 MHz) of **2** in $CDCl_3$

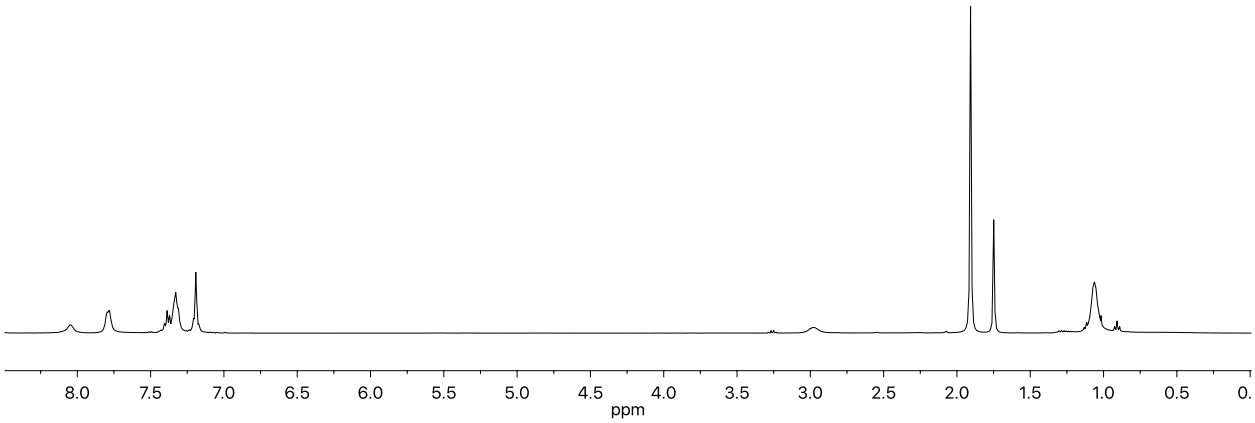


**Figure S3.** $^{1}$H NMR spectrum (400 MHz) of **3** in $C_6D_6$

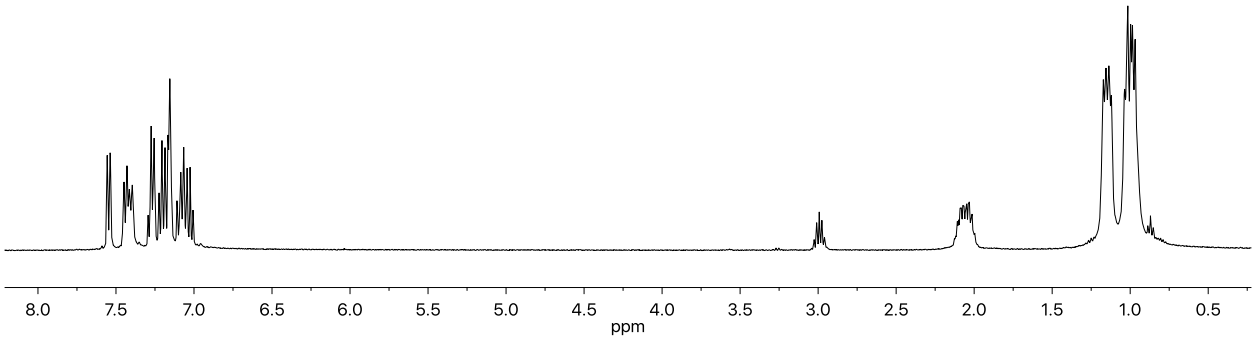


**Figure S4.** $^{1}$H NMR spectrum (400 MHz) of **5** in $C_6D_6$

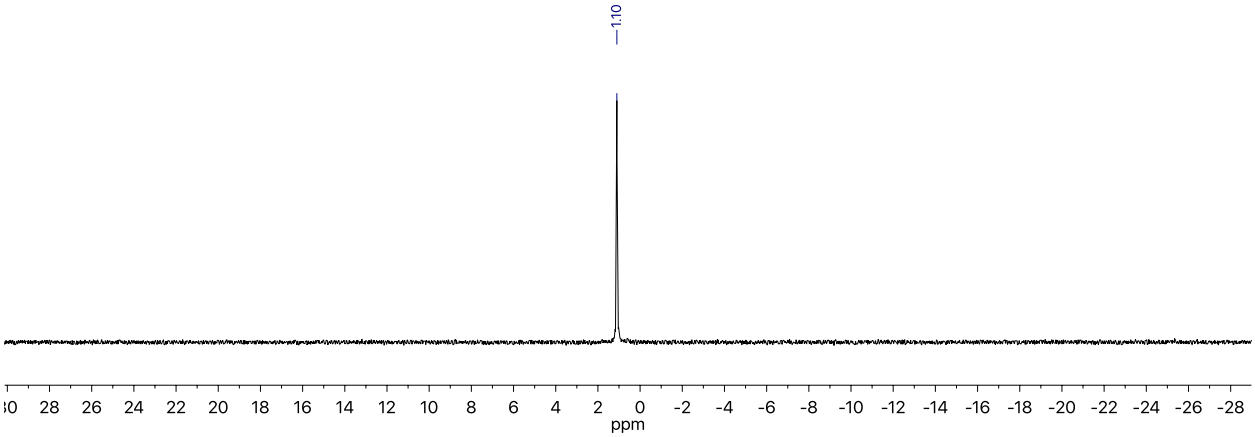


**Figure S5.** $^{31}$P NMR spectrum (162 MHz) of **5** in $C_6D_6$

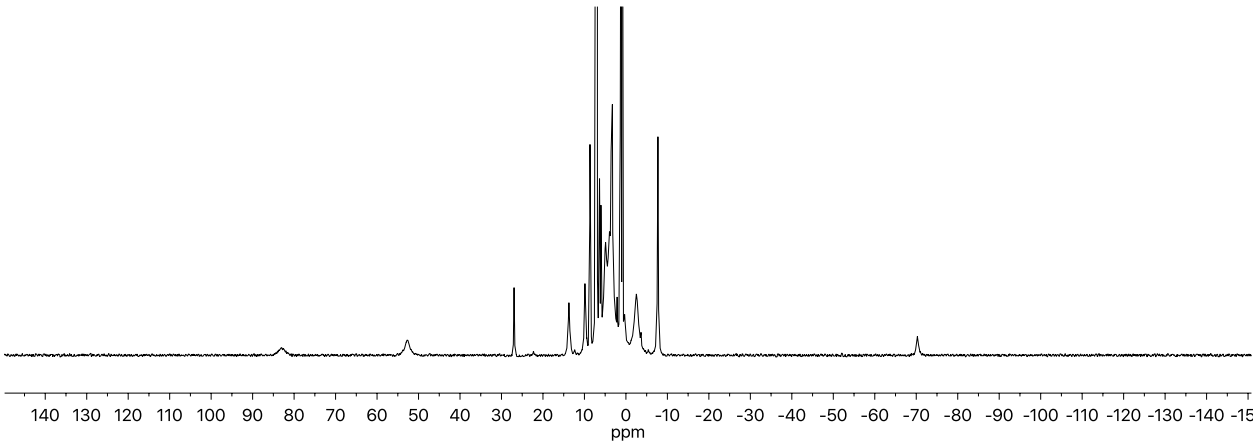


**Figure S6.** $^{1}$H NMR spectrum (300 MHz) of **6** in $C_6D_6$

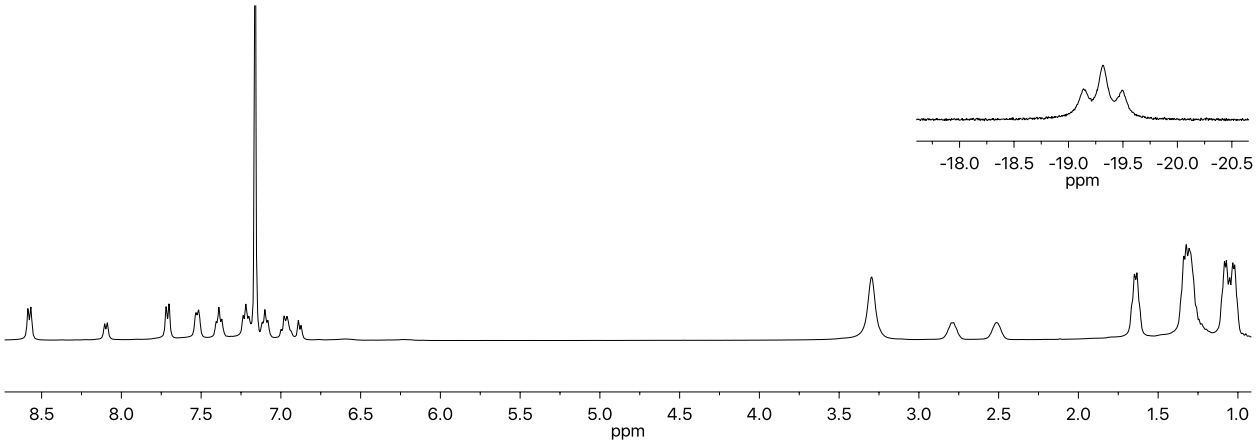


**Figure S7.** $^{1}$H NMR spectrum (300 MHz) of **7-H** in $C_6D_6$

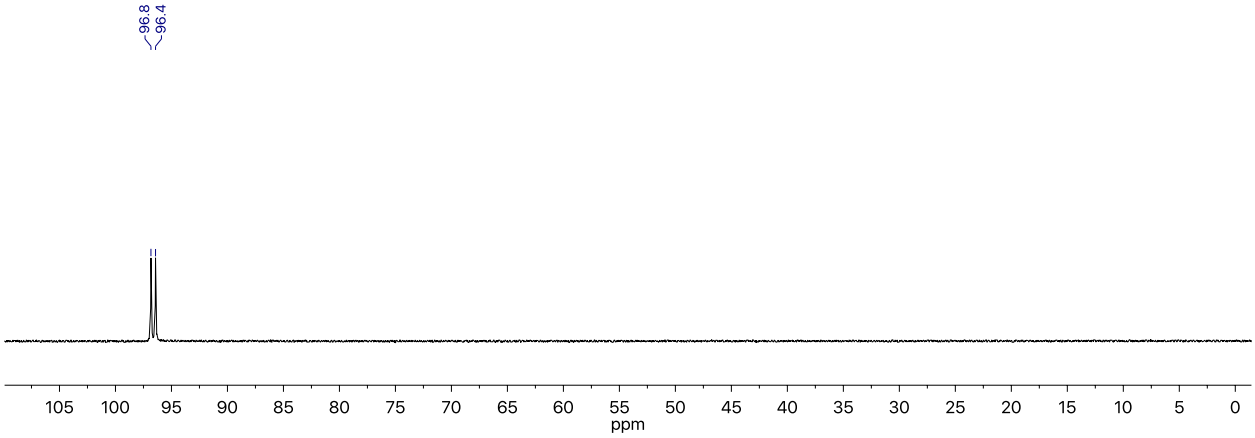


**Figure S8.** $^{31}$P NMR spectrum (162 MHz) of **7-H** in $C_6D_6$

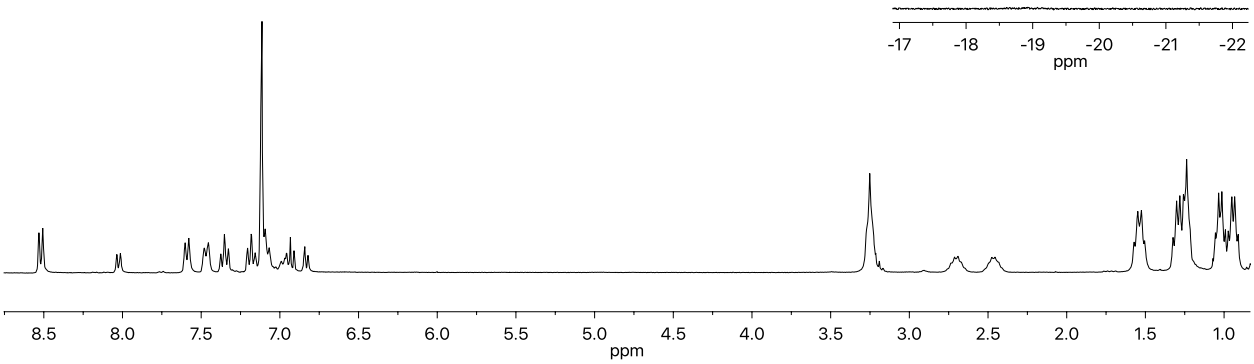


**Figure S9.** $^{1}H$ NMR spectrum (300 MHz) of **7-D** in $C_6D_6$

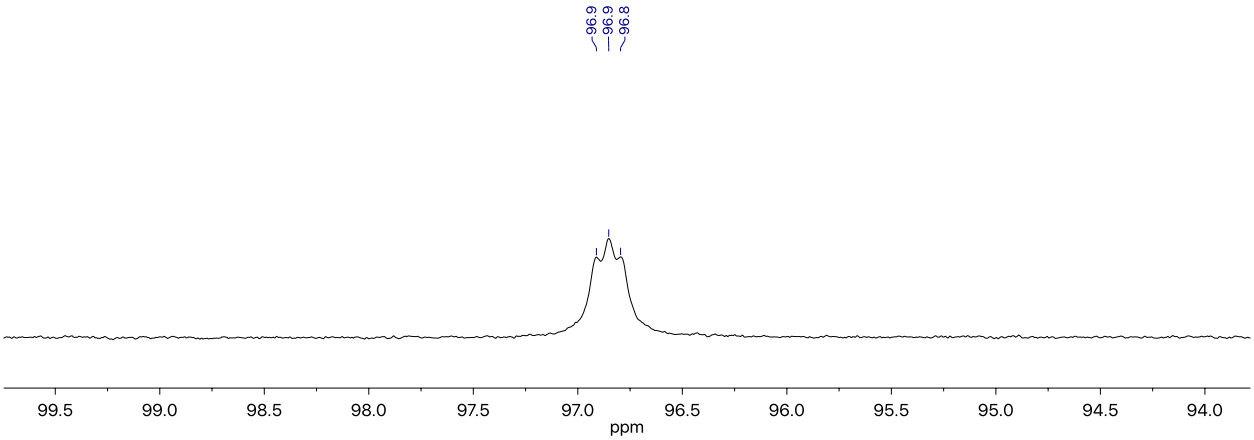


**Figure S10.** $^{31}P$ NMR spectrum (162 MHz) of **7-D** in $C_6D_6$

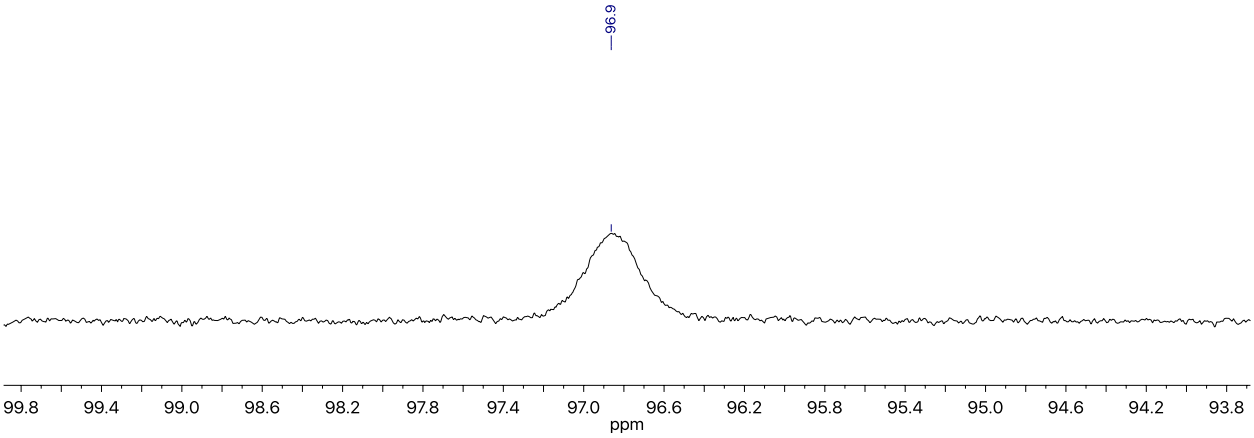


**Figure S11.** $^{31}P\{^{2}H\}$ NMR spectrum (162 MHz) of **7-D** in $C_6D_6$

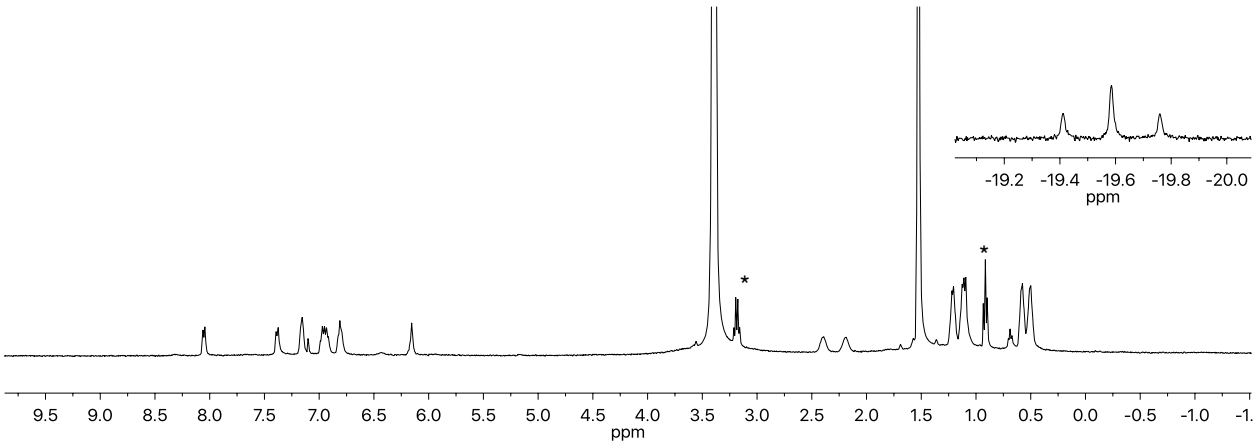


**Figure S12.** $^{1}$H NMR spectrum (400 MHz) of **7-H(crown)** in THF-$d_8$ (*$Et_2O$)

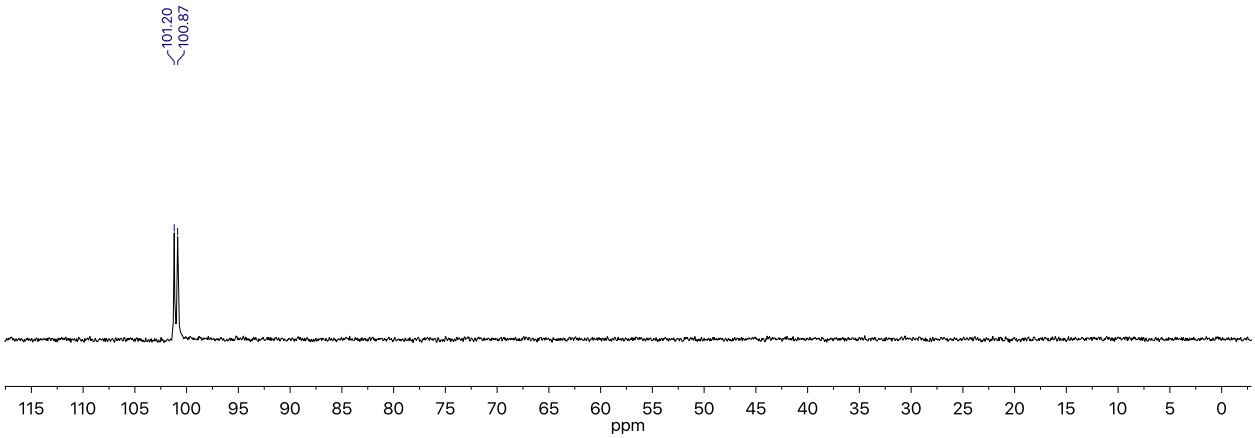


**Figure S13.** $^{31}$P NMR spectrum (162 MHz) of **7-H(crown)** in THF-$d_8$

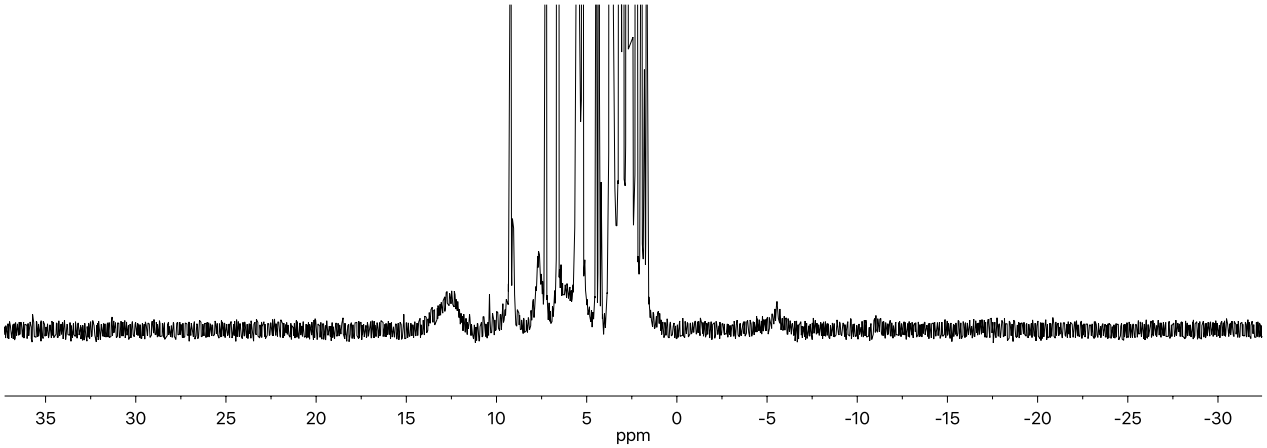


**Figure S14.** $^{1}$H NMR spectrum (500 MHz) of **8-H** in THF-$d_8$ (-78 ºC; generated in the presence of one equivalent of $Cp_2Co$)

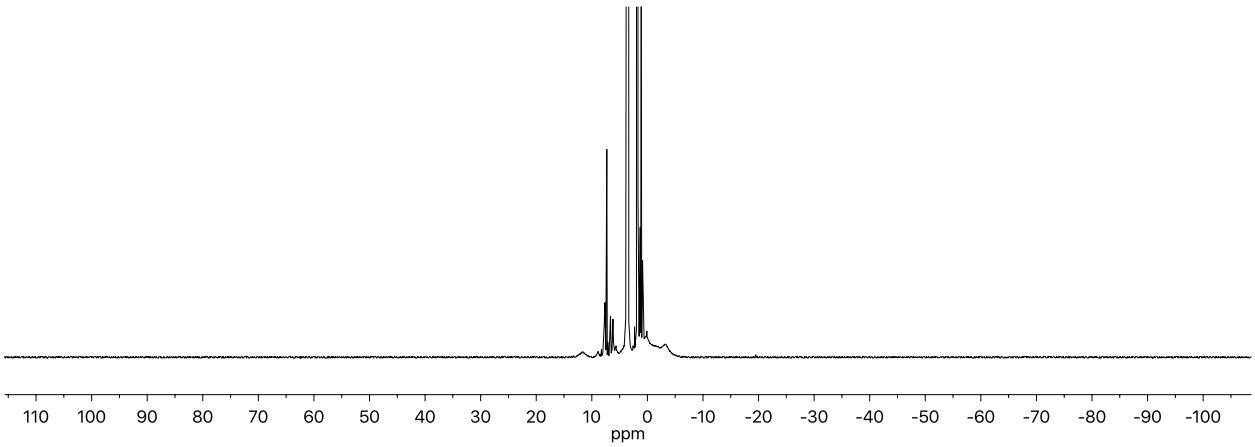


**Figure S15.** $^{1}$H NMR spectrum (400 MHz) of **9** in THF-$d_8$

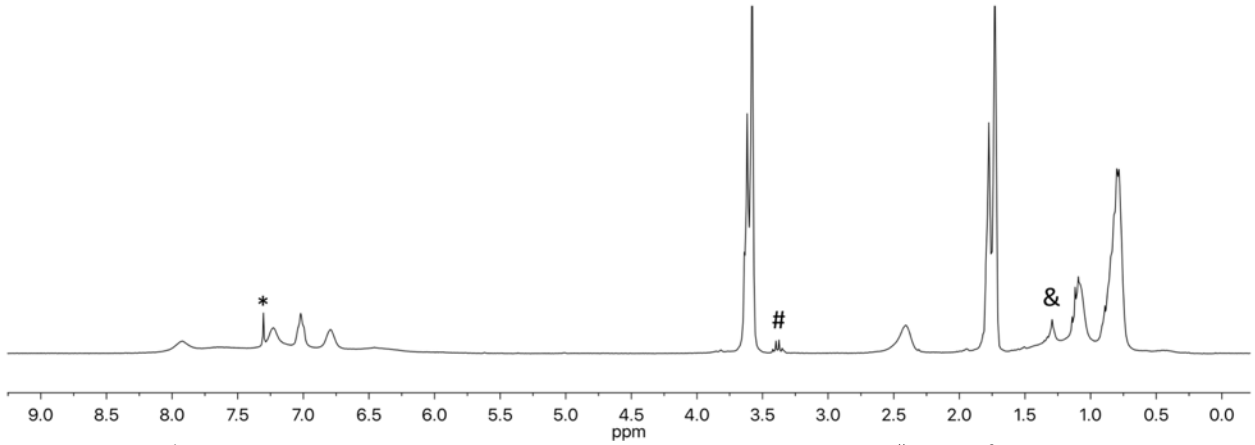


**Figure S16.** $^{1}$H NMR spectrum (300 MHz) of **10** in THF-$d_8$ (*$C_6H_6$, $^{\#}Et_2O$, $^{\&}$pentane)

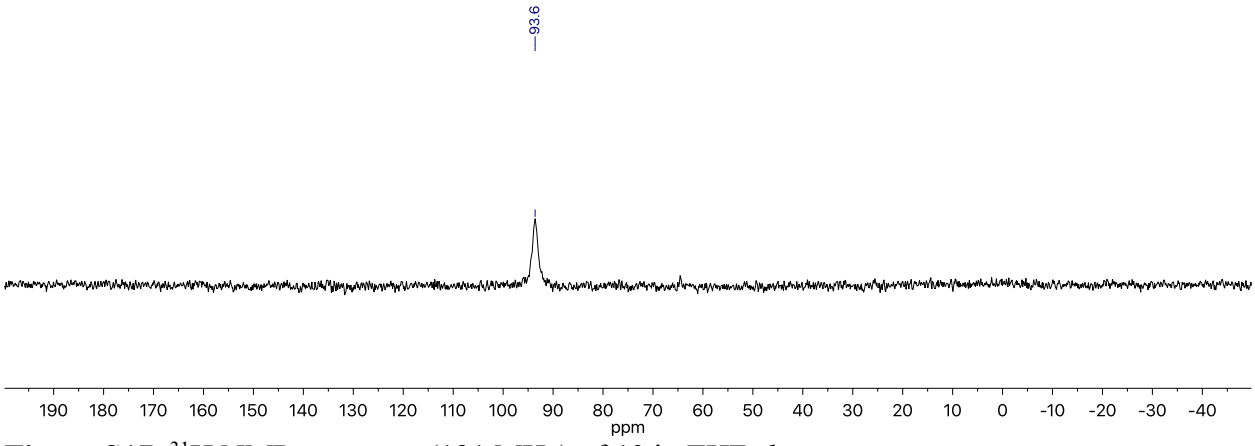


**Figure S17.** $^{31}$H NMR spectrum (121 MHz) of **10** in THF-$d_8$

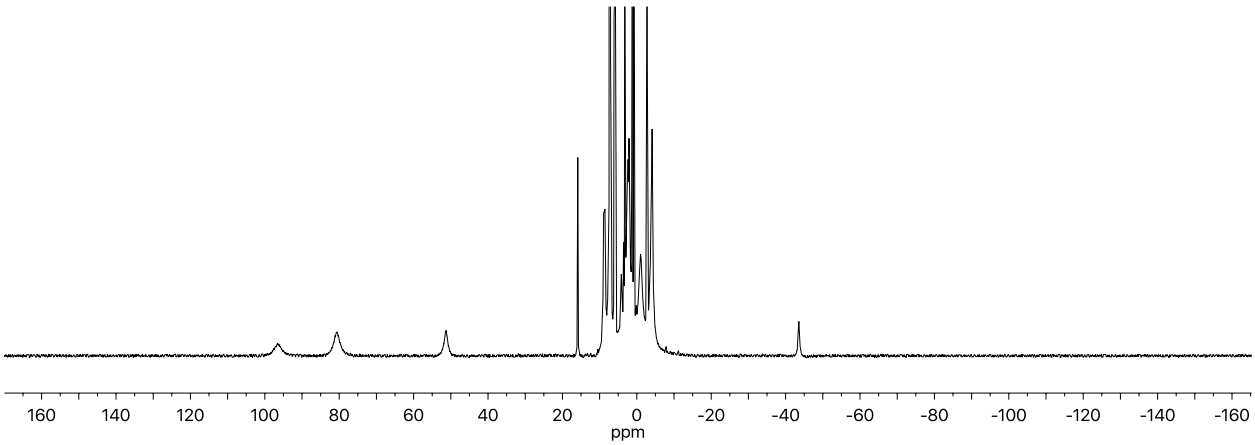


**Figure S18.** $^{1}$H NMR spectrum (400 MHz) of **11** in $C_6D_6$

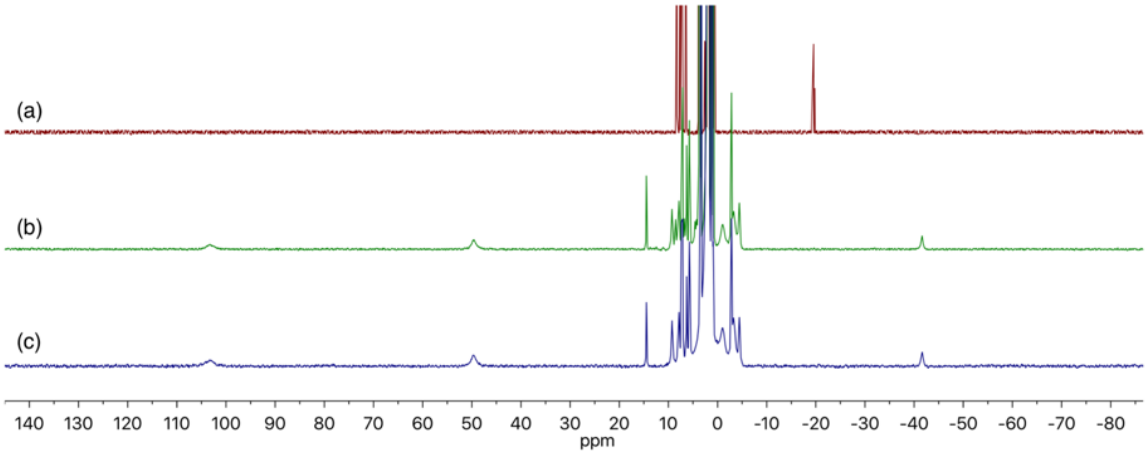


**Figure S19.** $^{1}$H spectra (300 MHz) of (a) complex **7-H(crown)** (b) reaction mixture of **7-H(crown)** under 1 atm of $CO_2$, collected 1 h after addition of $CO_2$ (c) complex **11** prepared from diiron **6**. All spectra collected in MeCN-$d_3$

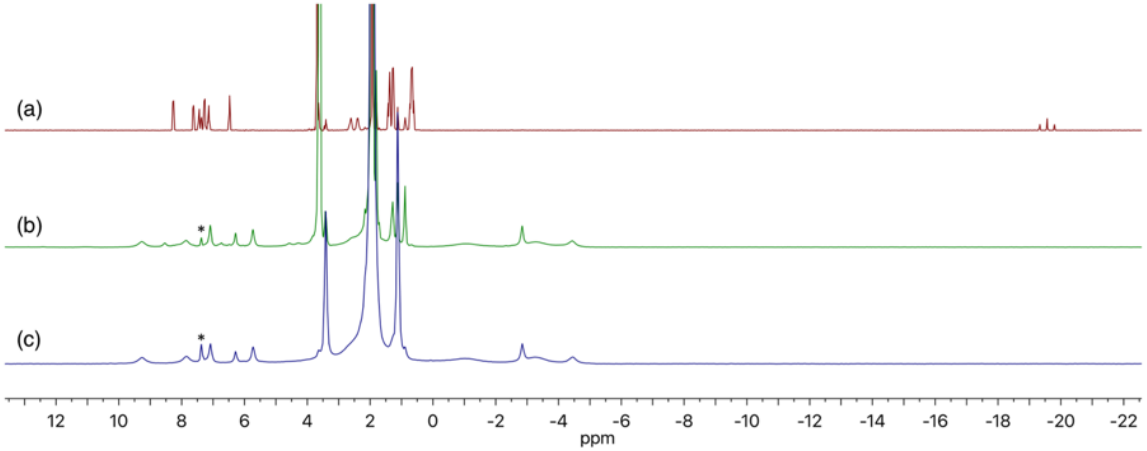


**Figure S20.** Partial $^{1}$H spectra (300 MHz) of (a) complex **7-H(crown)** (b) reaction mixture of **7-H(crown)** under 1 atm of $CO_2$, collected 1 h after addition of $CO_2$ (c) complex **11**. All spectra collected in MeCN-$d_3$ (* = $C_6H_6$)

*IR spectra*

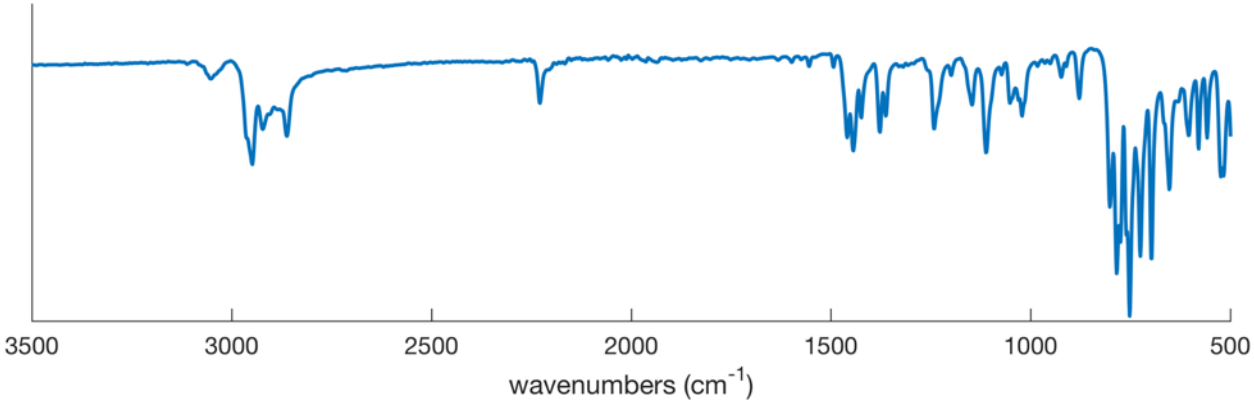


**Figure S21.** IR spectrum of **5** (solid powder sample)

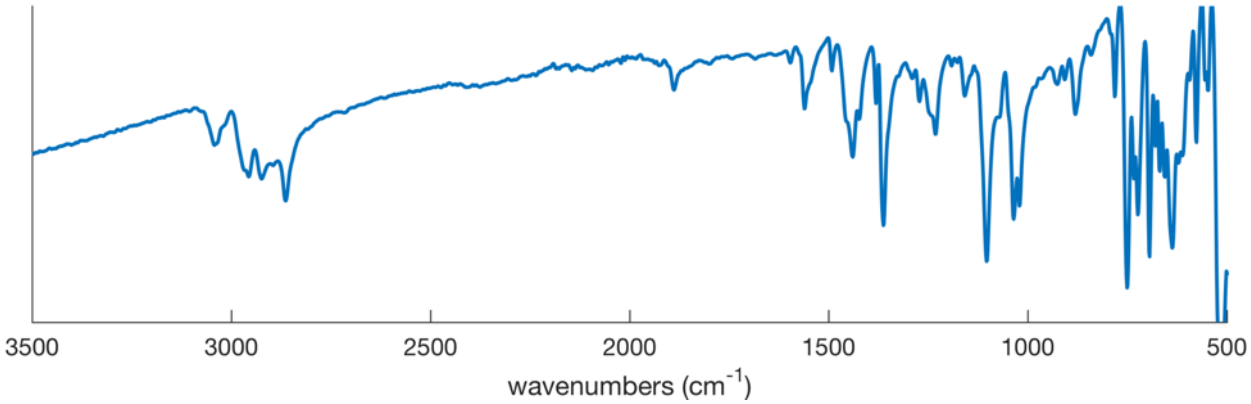


**Figure S22**. IR spectrum of **6** (solid crystalline sample)

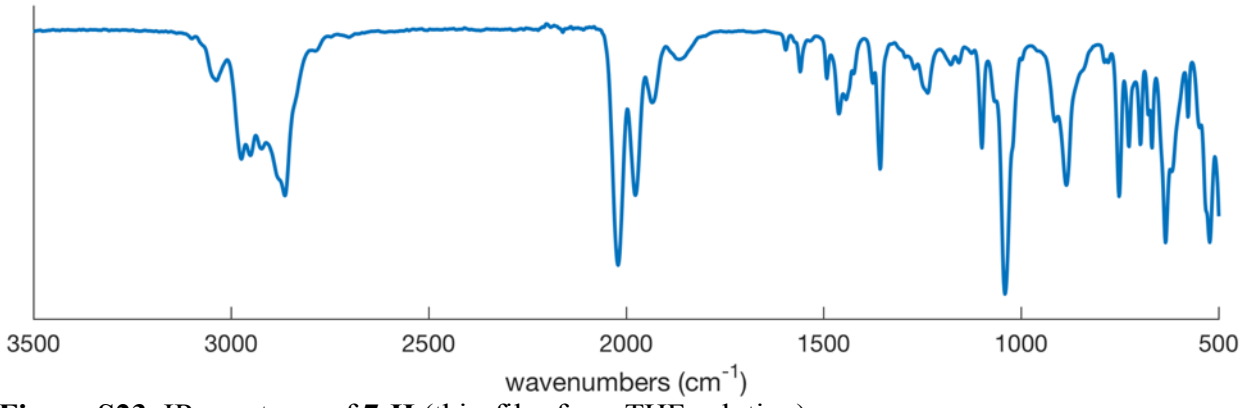


**Figure S23.** IR spectrum of **7-H** (thin-film from THF solution)

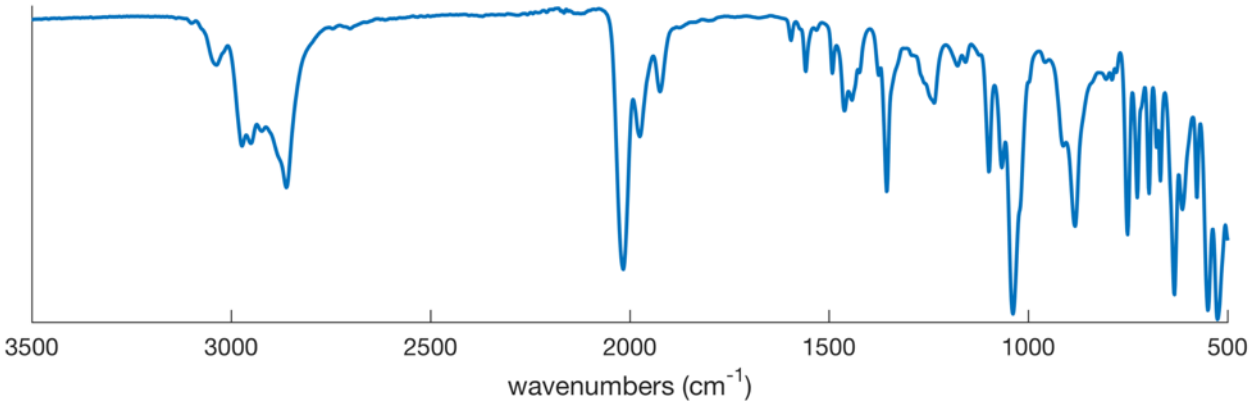


**Figure S24.** IR spectrum of **7-D** (thin-film from THF solution)

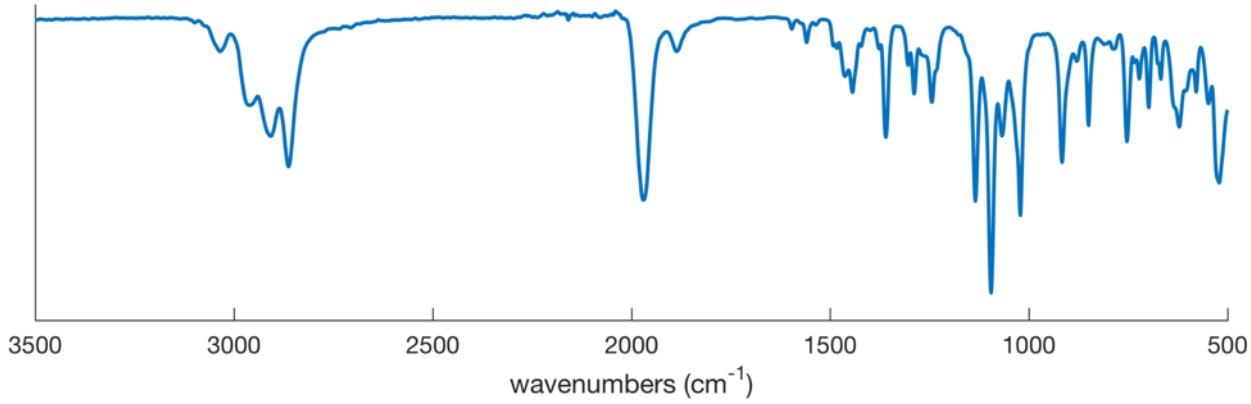


**Figure S25.** IR spectrum of **7-H(crown)** (thin-film from THF solution)

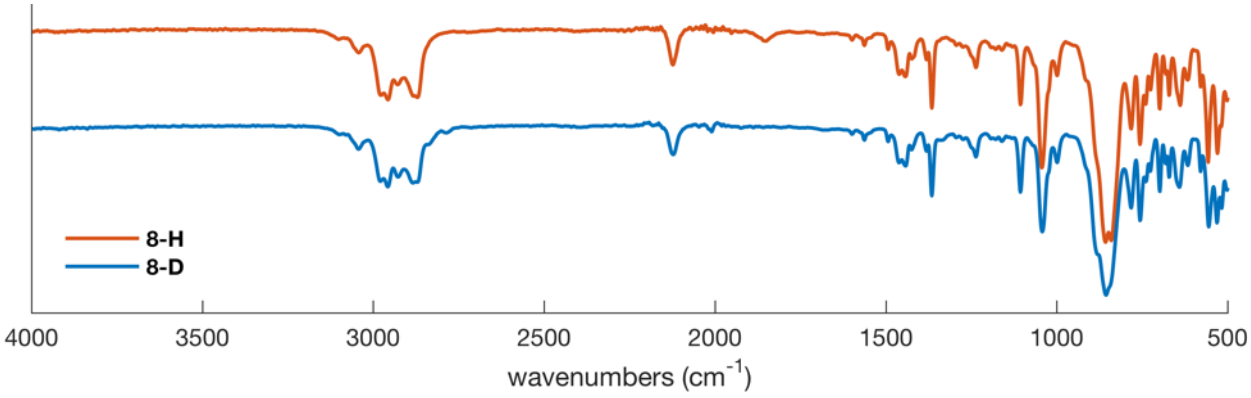


**Figure S26.** IR spectrum of **8-H** and **8-D** (thin-film from THF solution; generated in the presence of one equivalent of $Cp_2Co$)

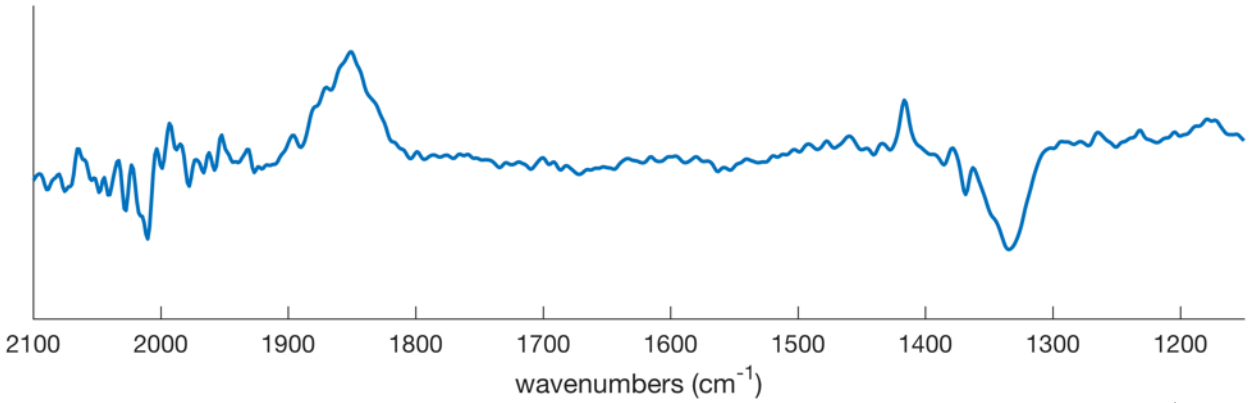


**Figure S27**. IR difference spectrum of **8-H** and **8-D** exhibiting an Fe-D stretch at 1333 $cm^{-1}$ and Fe-H stretch at 1852 $cm^{-1}$

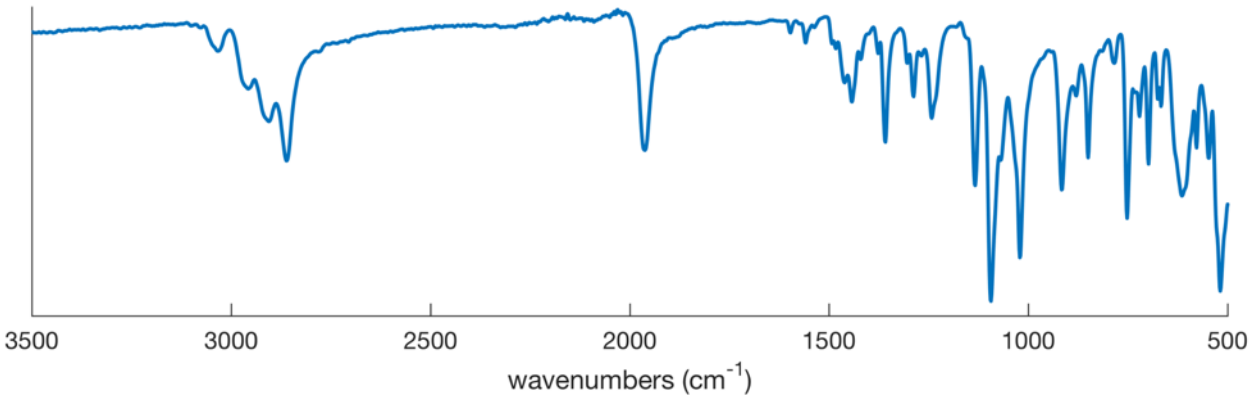


**Figure S28.** IR spectrum of **9** (solid crystalline sample)

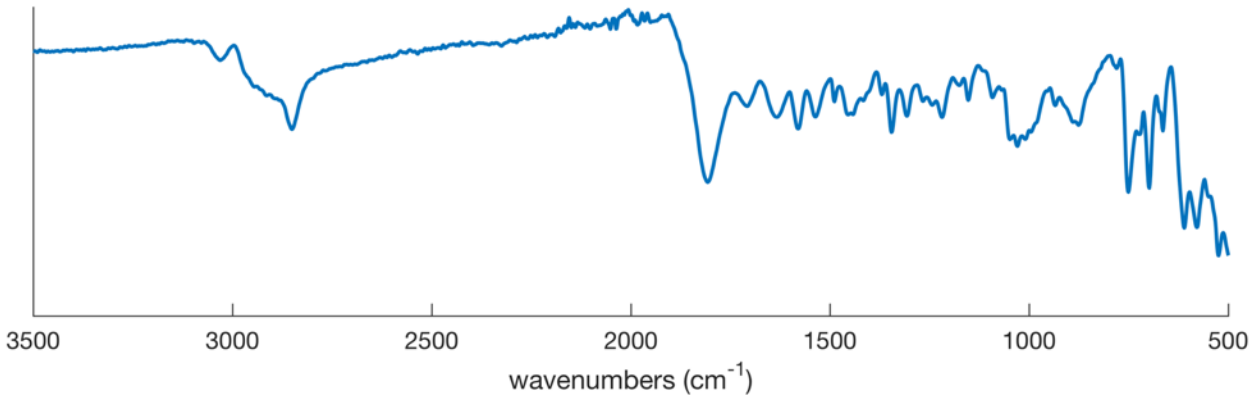


**Figure S29.** IR spectrum of **10** (solid powder sample)

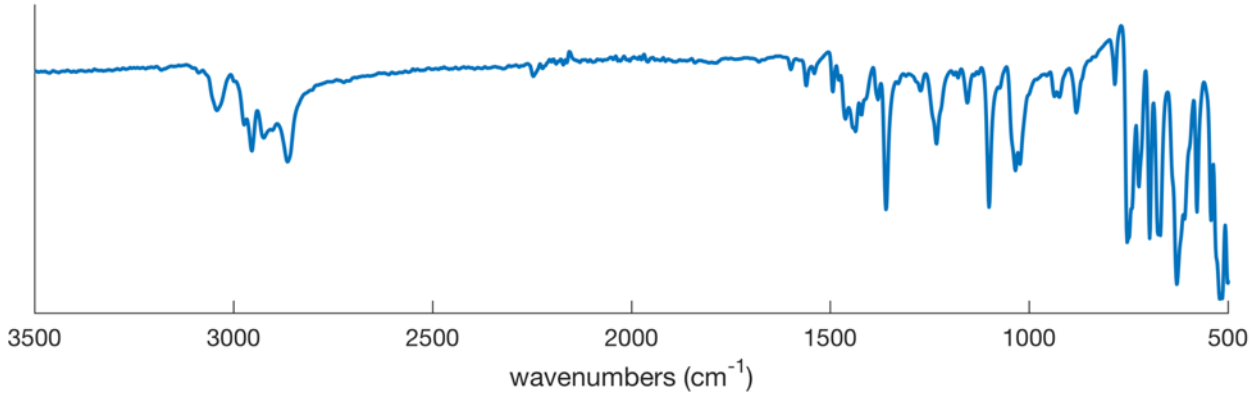


**Figure S30.** IR spectrum of **11** (solid powder sample)

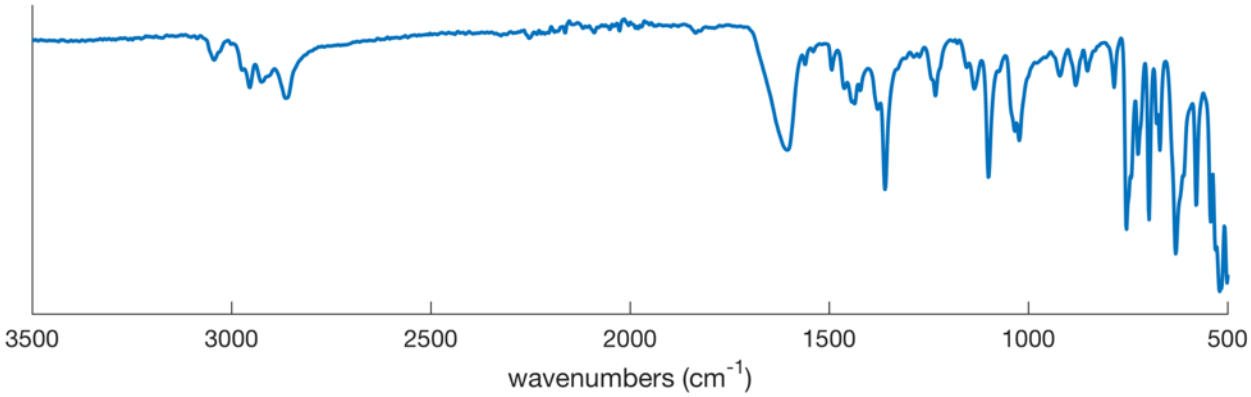


**Figure S31**. IR spectrum of the reaction of **7-H(crown)** with $CO_2$ (solid powder sample)

*X-ray diffraction*

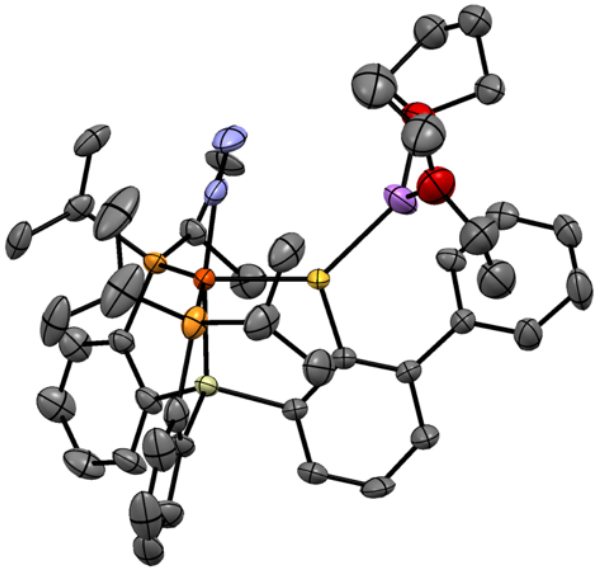

**Figure S32.** X-ray structure of **7-H**. Hydrogen and disordered atoms omitted for clarity. Ellipsoids shown at 50 % probability. Partial substitution of diethyl ether in place of THF was observed with regards to the solvent coordination at lithium, due to the crystals being grown from a diethyl ether solution.

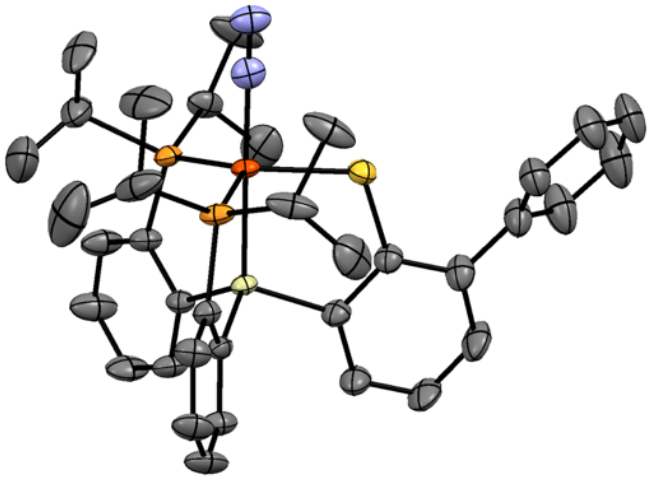

**Figure S33.** Structure of **9** with omission of countercation, disordered components, hydrogen atoms and solvent molecules. Thermal ellipsoids at 50% probability.

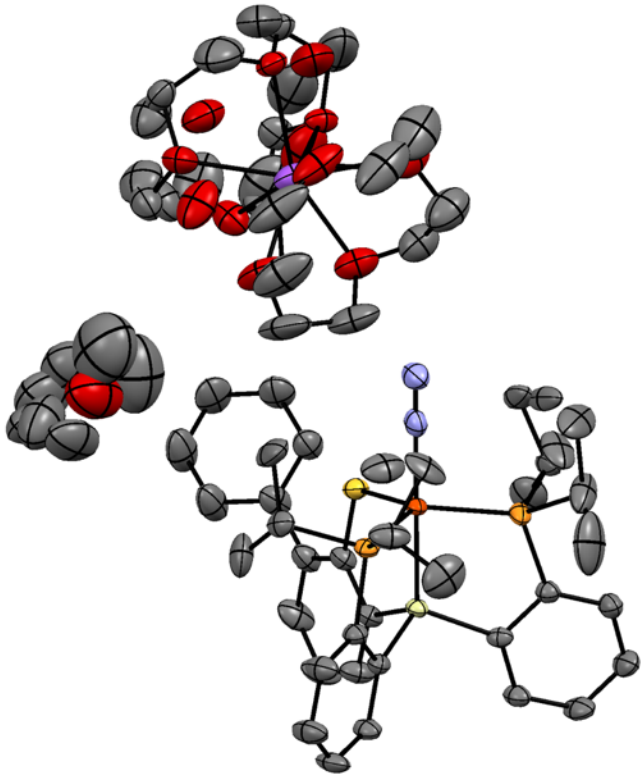

**Figure S34.** Full asymmetric unit of **9** including solvent and disordered components. Hydrogen atoms omitted; thermal ellipsoids at 50% probability.

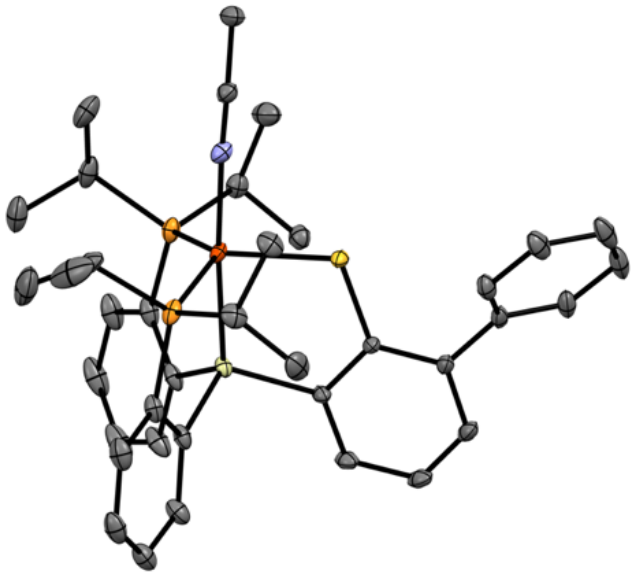

**Figure S35.** Structure of **11** with omission of disordered components and hydrogen atoms. Thermal ellipsoids at 50% probability.

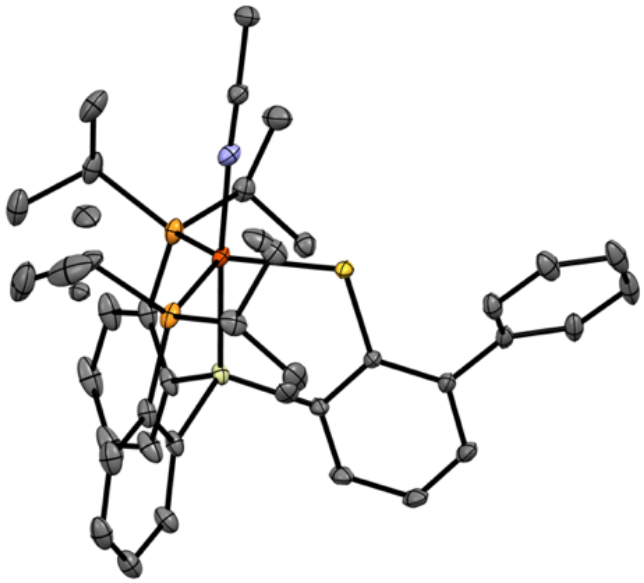

**Figure S36.** Full asymmetric unit of **11** including disordered components. Hydrogen atoms omitted; thermal ellipsoids at 50% probability.

*$^{57}$Fe Mössbauer spectra*

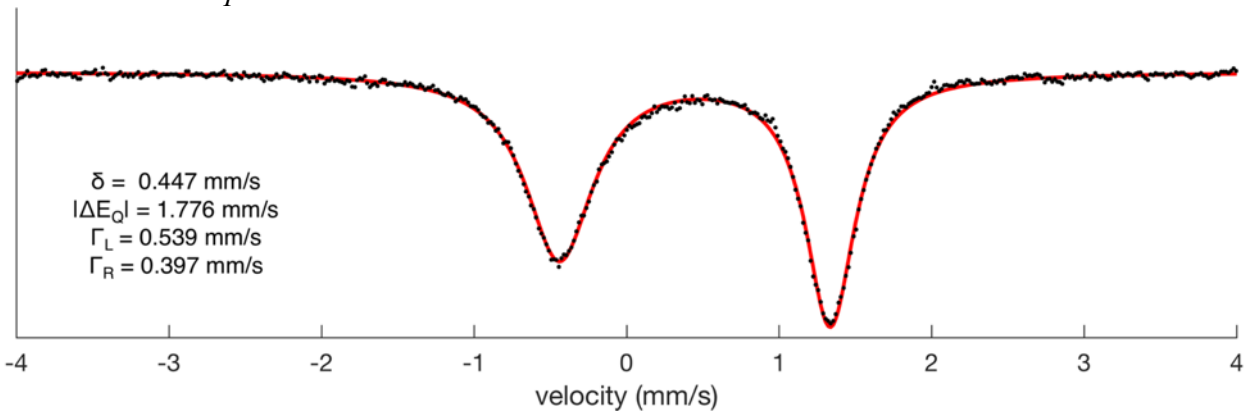


**Figure S37.** 80K $^{57}$Fe Mössbauer spectrum of **6** collected in the presence of a 50 mT magnetic field oriented parallel to the propagation of the γ-beam (solid sample suspended in boron nitride)

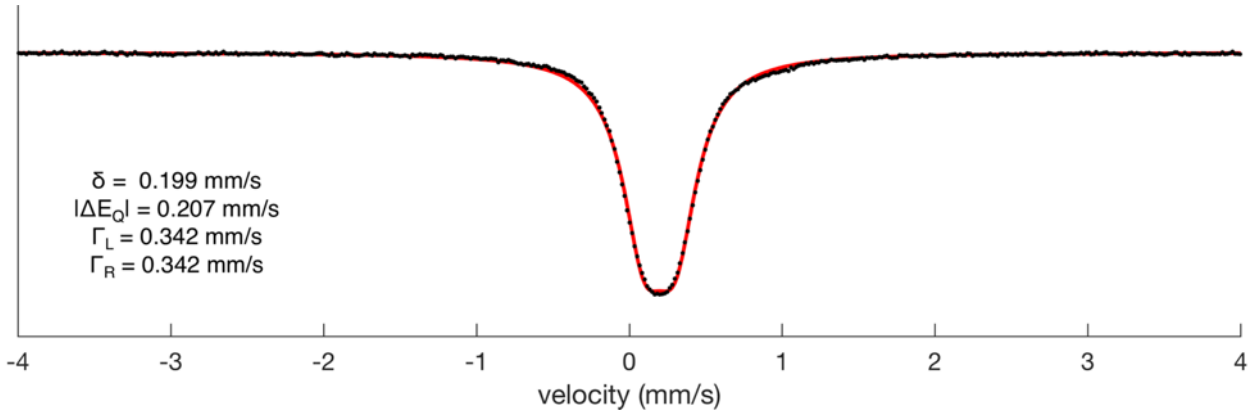


**Figure S38.** 80 K $^{57}$Fe Mössbauer spectrum of **7-H** collected in the presence of a 50 mT magnetic field oriented parallel to the propagation of the γ-beam (frozen solution sample in THF)

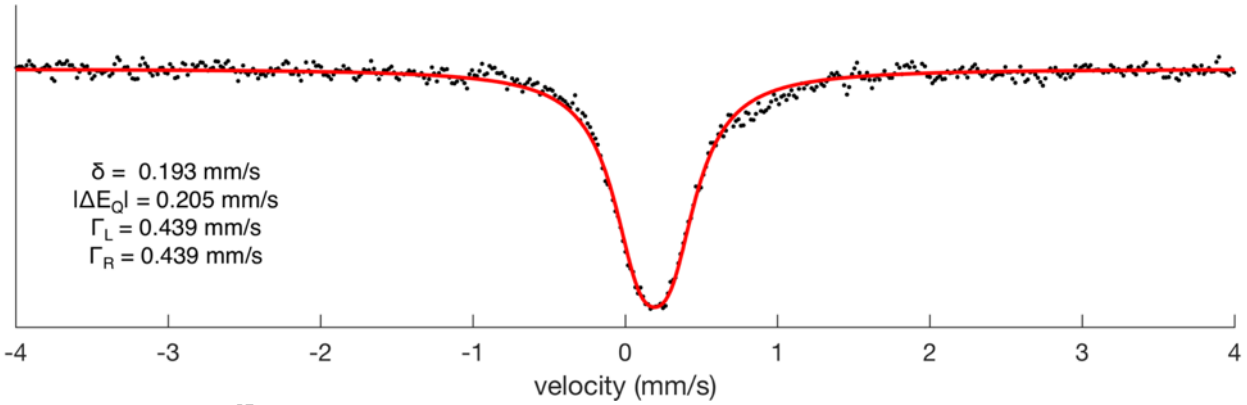


**Figure S39.** 80K $^{57}$Fe Mössbauer spectrum of **7-H(crown)** collected in the presence of a 50 mT magnetic field oriented parallel to the propagation of the γ-beam (solid sample suspended in boron nitride)

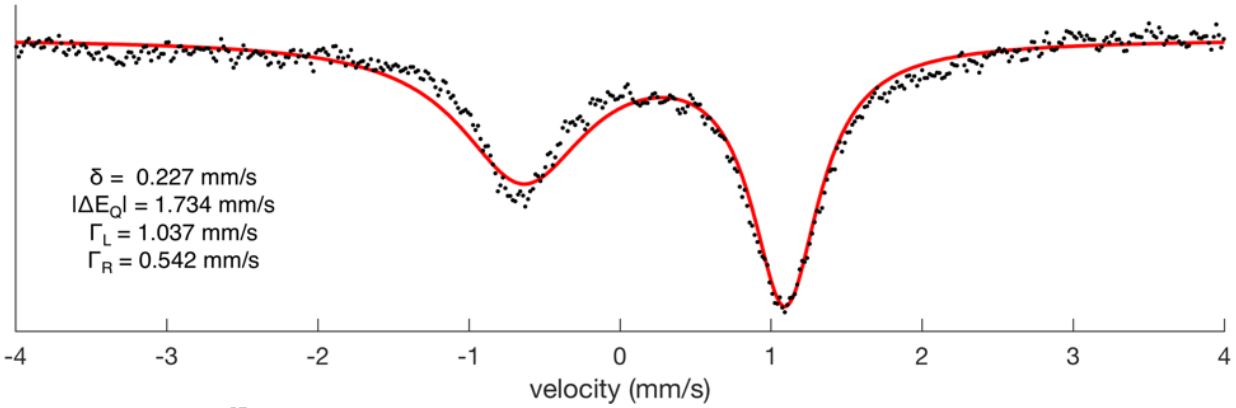


**Figure S40.** 80K $^{57}$Fe Mössbauer spectrum of **8-H** collected in the presence of a 50 mT magnetic field oriented parallel to the propagation of the γ-beam (solid sample suspended in boron nitride; generated in the presence of one equivalent of $Cp_2Co$)

*EPR spectra*

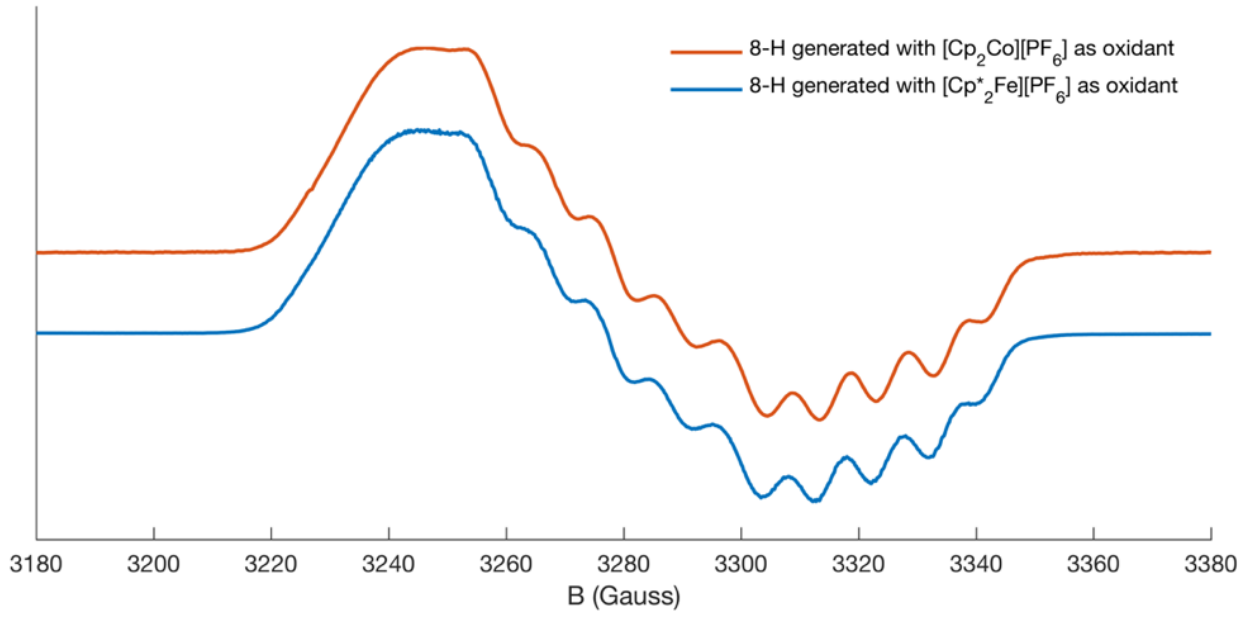


**Figure S41.** 77 K X-band EPR spectra of **8-H** in 2-MeTHF, generated with $[Cp_2Co][PF_6]$ and $[Cp^*_2Fe][PF_6]$ as oxidants

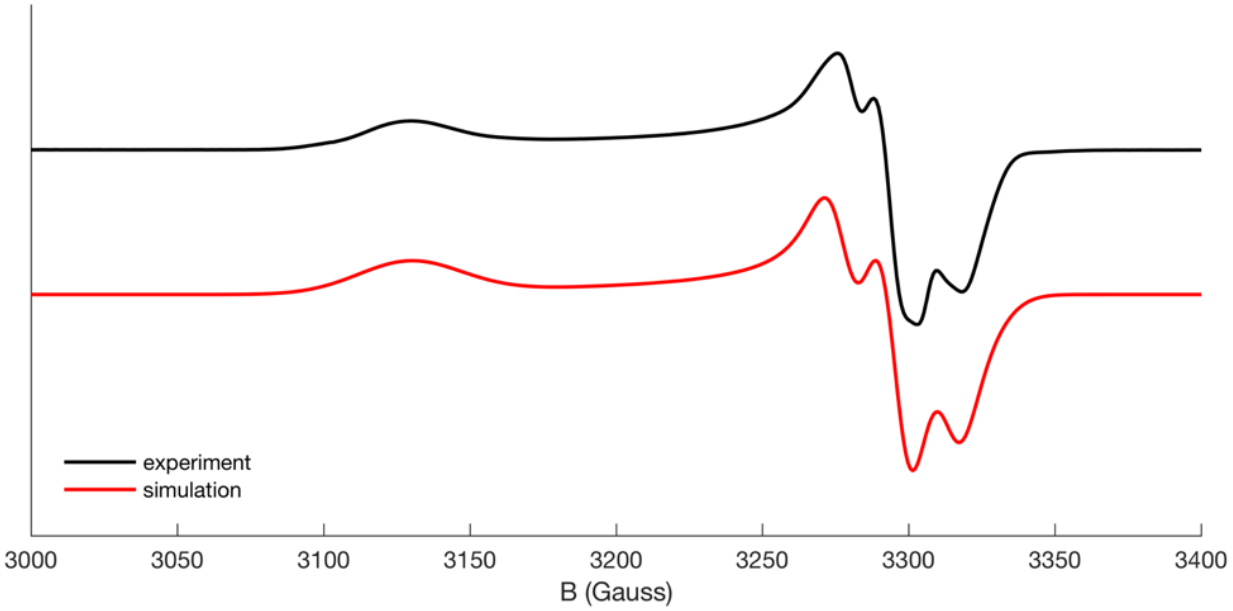


**Figure S42.** 77K K X-band EPR spectra of **9** in 2-MeTHF with simulation (Sys.g = [2.1440 2.0350 2.0300], Sys.lw = 1.2, Sys.Nucs = '31P, 31P', Sys.A = [0 50 45; 0 50 45], Sys.HStrain = [120 0 60], Exp.mwFreq = 9.389)

*ENDOR spectroscopy*

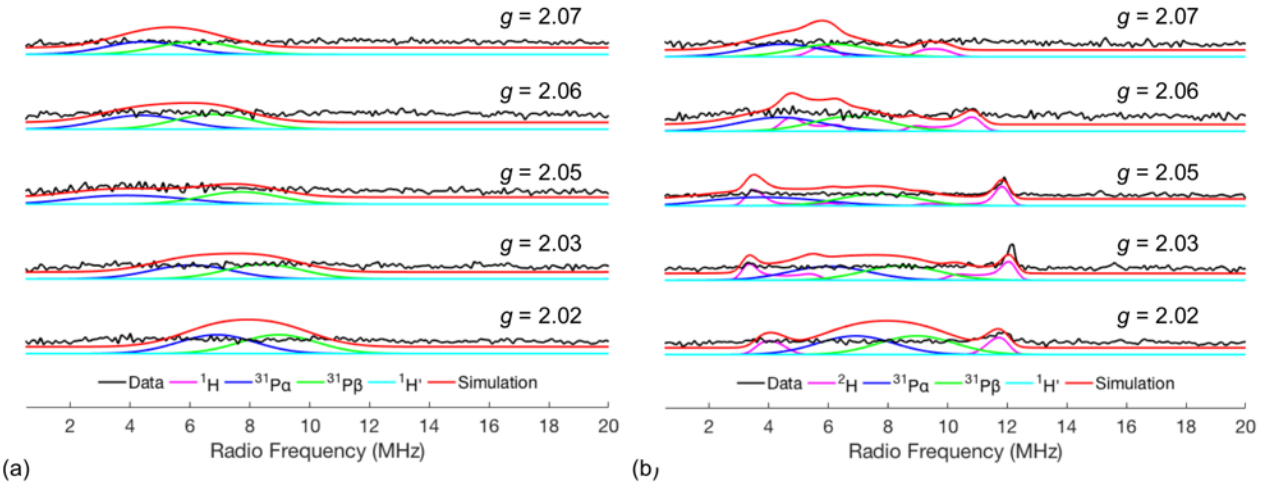


**Figure S43.** Field-dependent Q-band Davies ENDOR of (a) **8-H** and (b) **8-D** in 2Me-THF with simulations (partial spectrum of Fig. 4ab). Simulation parameters: **g** = [2.07, 2.0475, 2.02]; **A**($^{31}$P$\alpha$) = ±[31, 36, 27] MHz; **A**($^{31}$P$\beta$) = ±[28, 25, 23] MHz; **A**($^{1}$H') = ±[6.8, 10, 6.8] MHz. Fig. S43a was simulated with additional coupling to Fe-*H* (**A**($^{1}$H) = ±[15, 56, 58] MHz), whereas Fig. S43b was simulated with additional coupling to Fe-*D* (**A**($^{2}$H) = ±[2.3, 8.6, 8.9] MHz). Summation of individual component ENDOR simulations is displayed in red. Experimental conditions: microwave frequency = 33.674 GHz; MW π pulse length = 40 ns; interpulse delay τ = 300 ns; $\pi_{RF}$ pulse length = 15 µs; TRF delay = 1 µs; shot repetition time (srt) = 5 ms; temperature = 18.5 K;

RF frequency randomly sampled. The simulated $^{31}P$ signals at lower frequencies have very low intensity in the experimental data, possibly as a product of the hyperfine enhancement effect and lower RF magnetic field intensity generated by the ENDOR coils at very low frequencies.

*UV-Visible spectra*

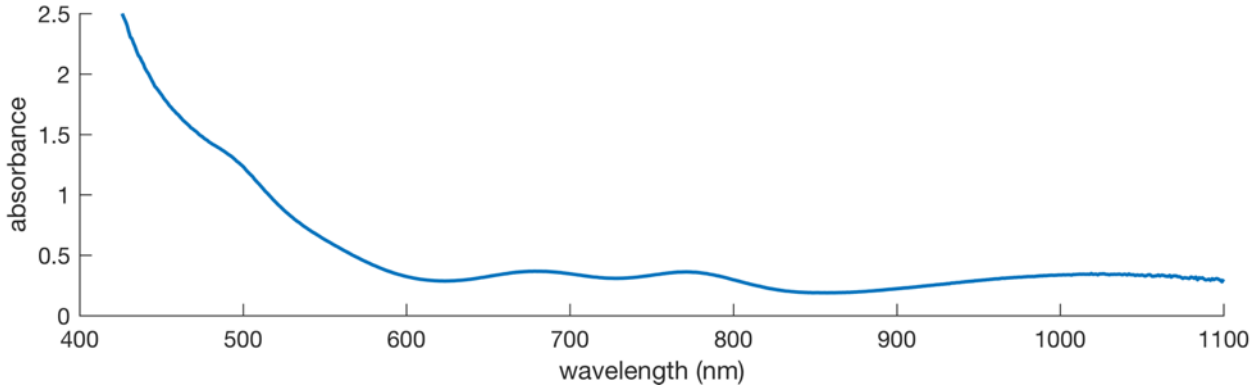


**Figure S44.** UV-Vis spectrum of **6** in THF

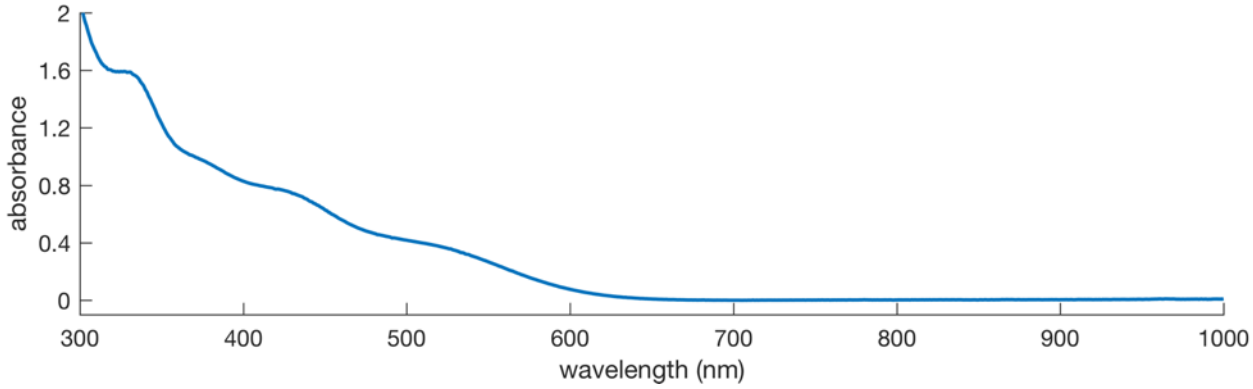


**Figure S45.** UV-Vis spectrum of **7-H** in THF

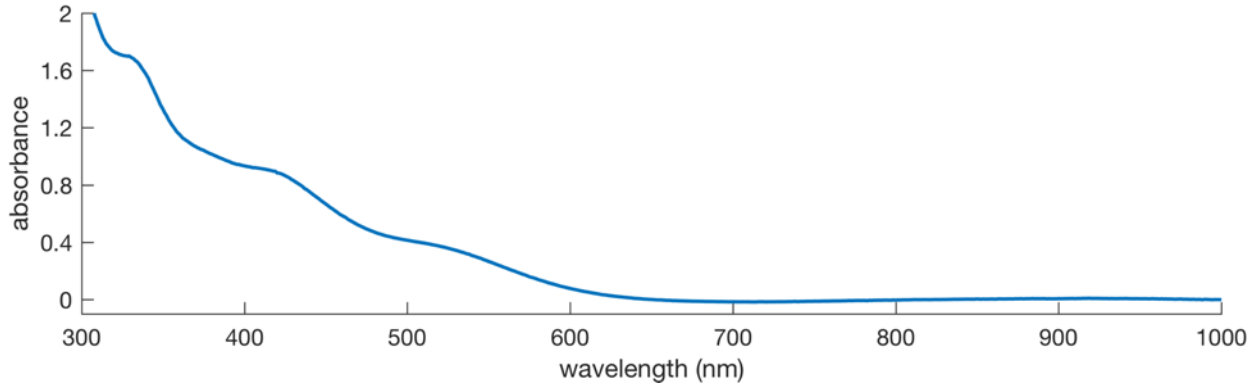


**Figure S46.** UV-Vis spectrum of **7-H(crown)** in THF

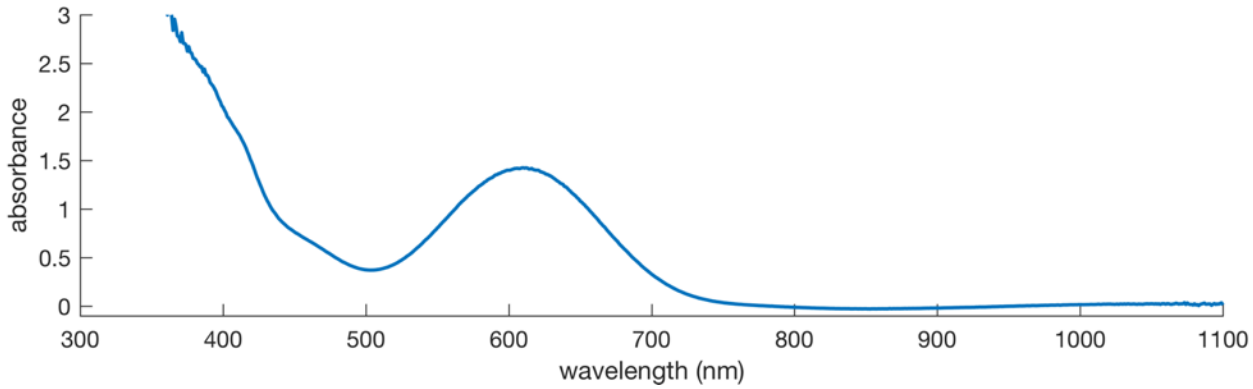


**Figure S47.** UV-Vis spectrum of **8-H** in THF (1 mm cuvette, generated in the presence of one equivalent of $Cp_2Co$)

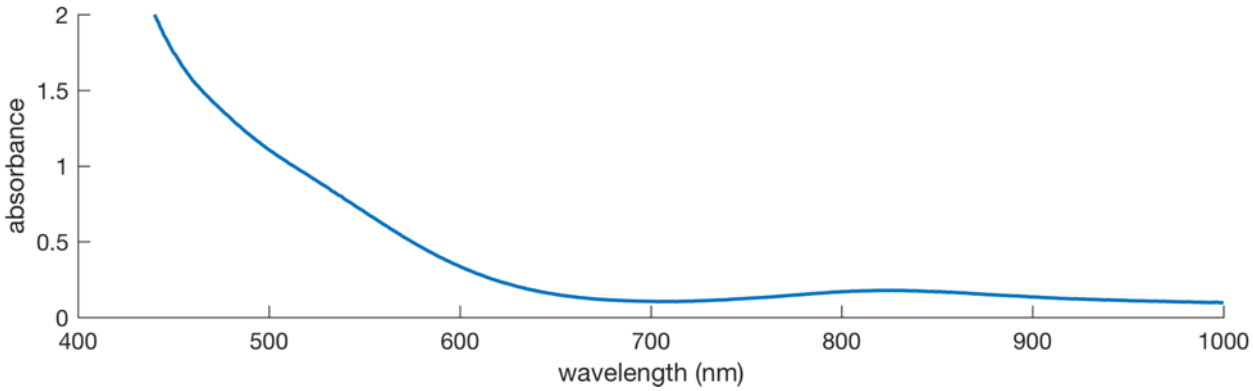


**Figure S48.** UV-Vis spectrum of **9** in THF

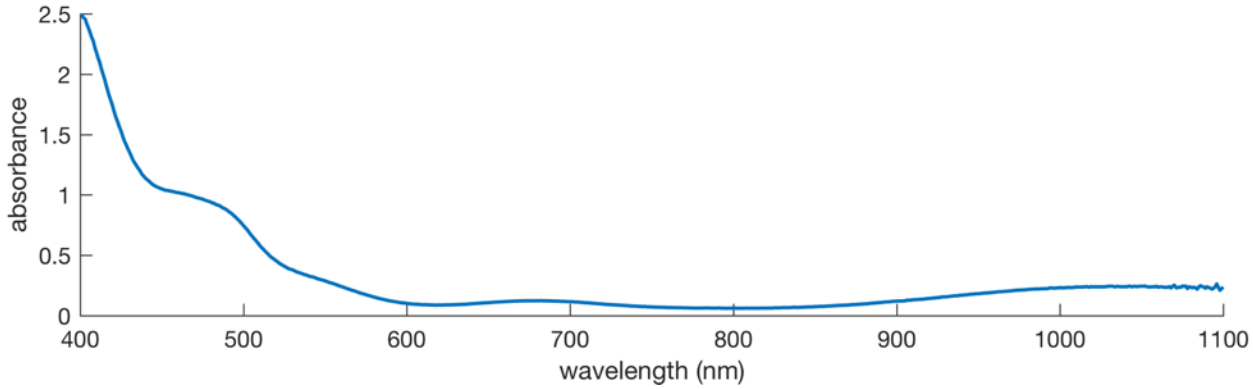


**Figure S49.** UV-Vis spectrum of **11** in THF

*Cyclic voltammograms*

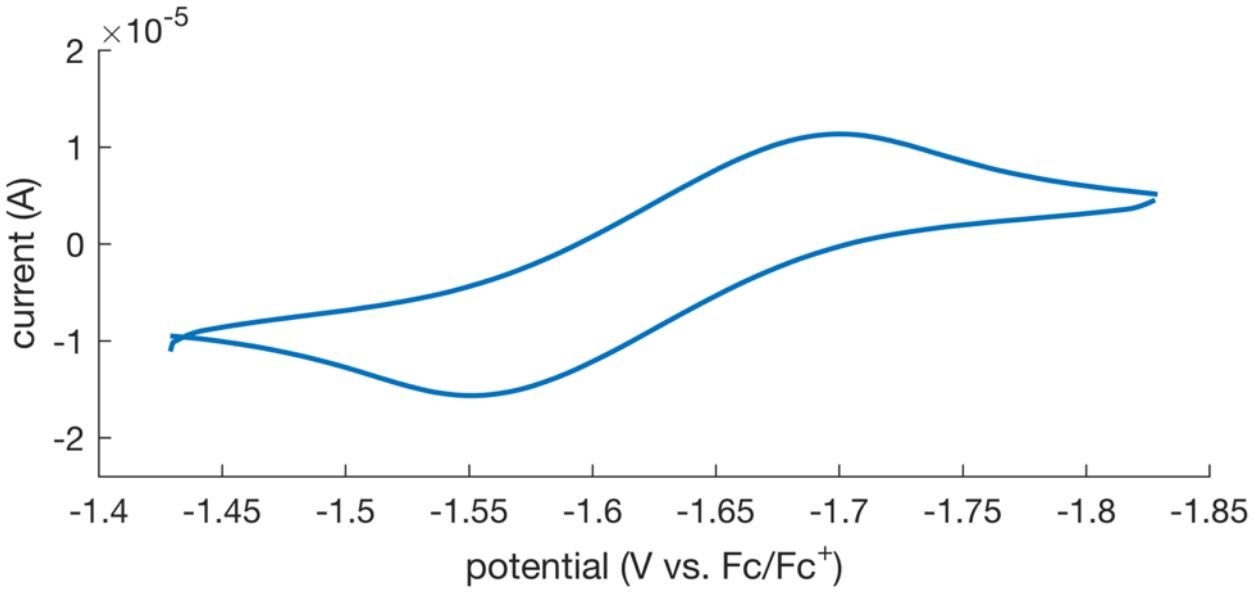


**Figure S50.** Cyclic voltammogram of **7-H(crown)** in THF (0.4 M [$NBu_4$][$PF_6$]) showing the reversible Fe(II)/Fe(III) couple centered at -1.63 V vs $Fc/Fc^+$. Data was collected at 400 mV/s with Pt counter, glassy carbon working and Ag/AgOTf reference electrodes

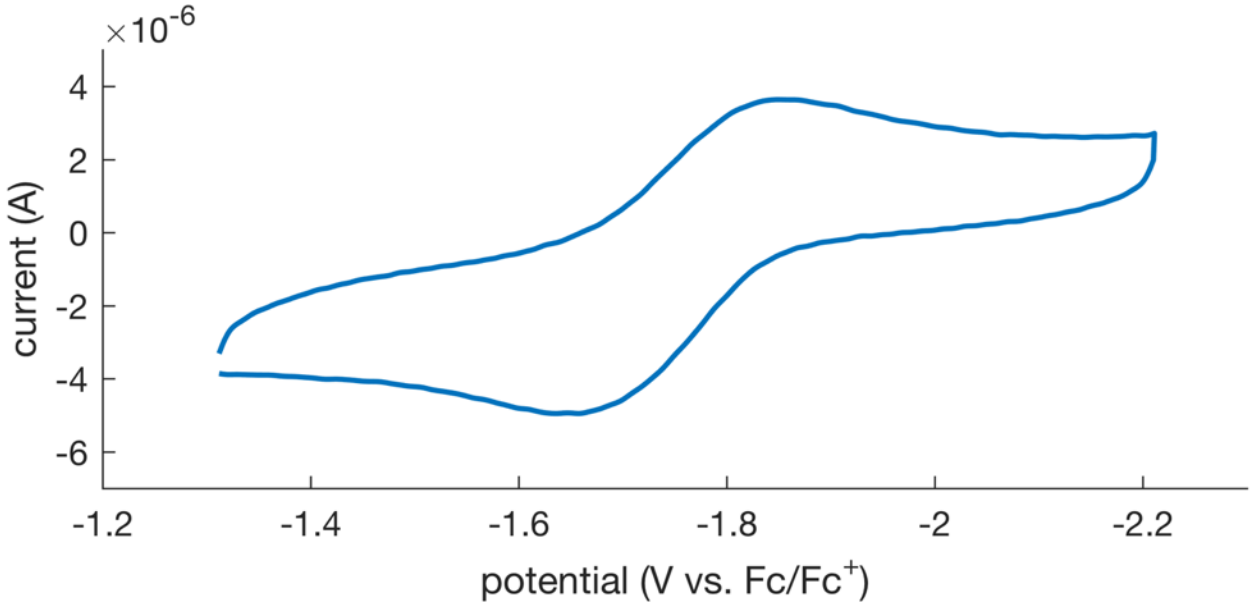


**Figure S51.** Cyclic voltammogram of **9** in THF (0.4 M [$NBu_4$][$PF_6$]) showing the reversible Fe(I)/Fe(II) couple centered at -1.75 V vs $Fc/Fc^+$. Data was collected at 400 mV/s with Pt counter, glassy carbon working and Ag/AgOTf reference electrodes

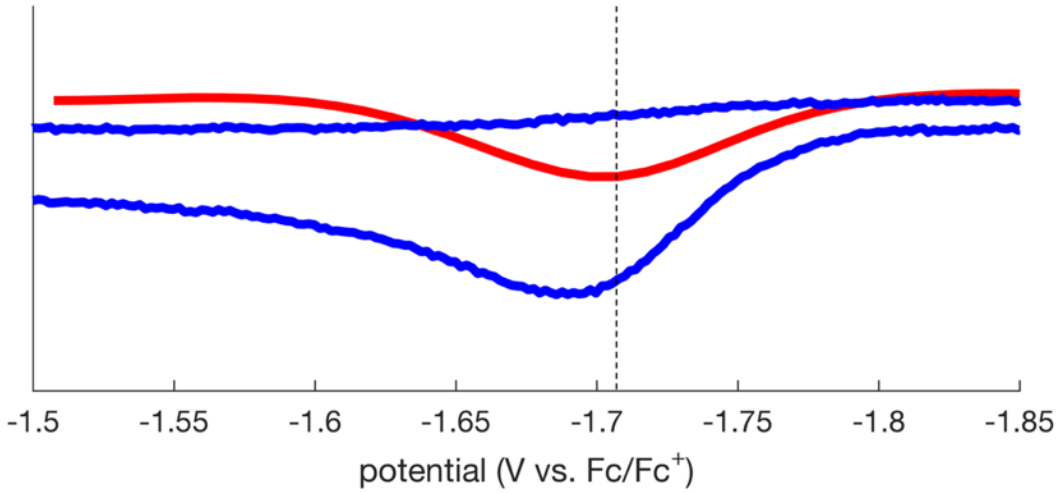


**Figure S52.** Cyclic voltammogram (blue) and square wave voltammogram (red) of **9** in MeCN (0.4 M $[NBu_4][PF_6]$) showing the irreversible Fe(I)/Fe(II) couple centered at -1.71 V vs. $Fc/Fc^+$. Data was collected at 100 mV/s with Pt counter, glassy carbon working and Ag/AgOTf reference electrodes

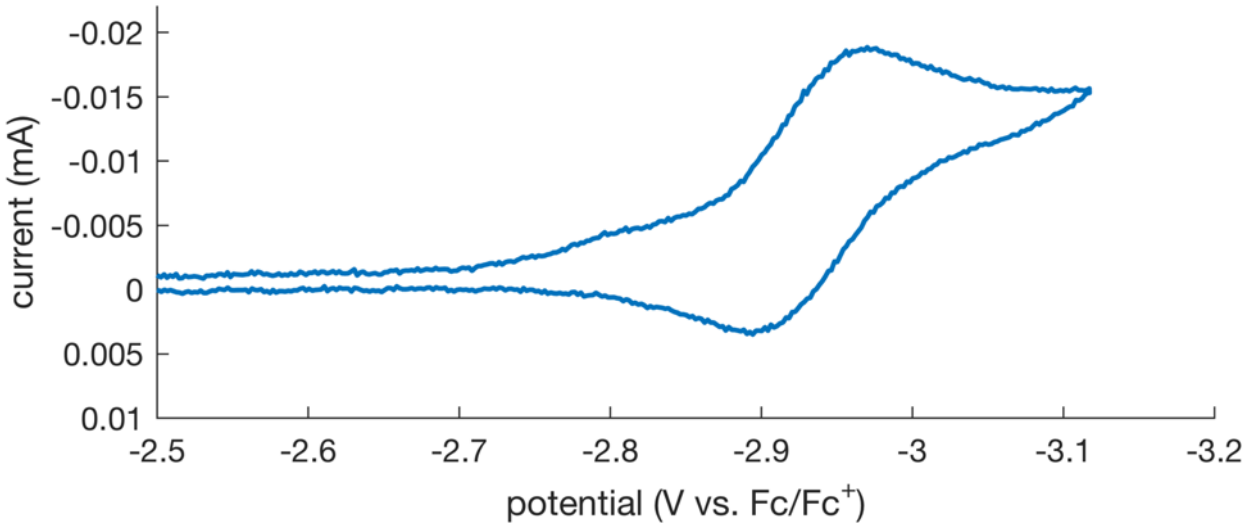


**Figure S53.** Cyclic voltammogram of **9** in MeCN (0.4 M $[NBu_4][PF_6]$) showing the reversible Fe(I)/Fe(0) couple centered at -2.94 V vs. $Fc/Fc^+$. Data was collected at 100 mV/s with Pt counter, glassy carbon working and Ag/AgOTf reference electrodes

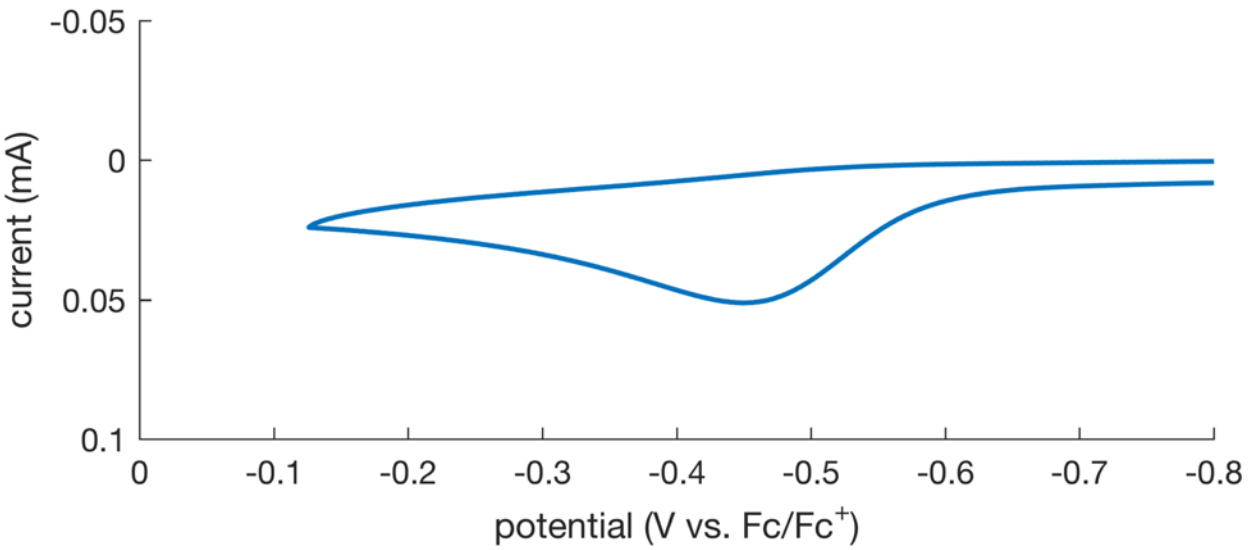


**Figure S54.** Cyclic voltammogram of **7-H(crown)** in MeCN (0.4 M [$NBu_4$][$PF_6$]) showing the reversible Fe(II)/Fe(III) couple with an onset at -0.58 V vs. $Fc/Fc^+$. Data was collected with Pt counter, glassy carbon working and Ag/AgOTf reference electrodes

*Variable temperature Evans method measurements*

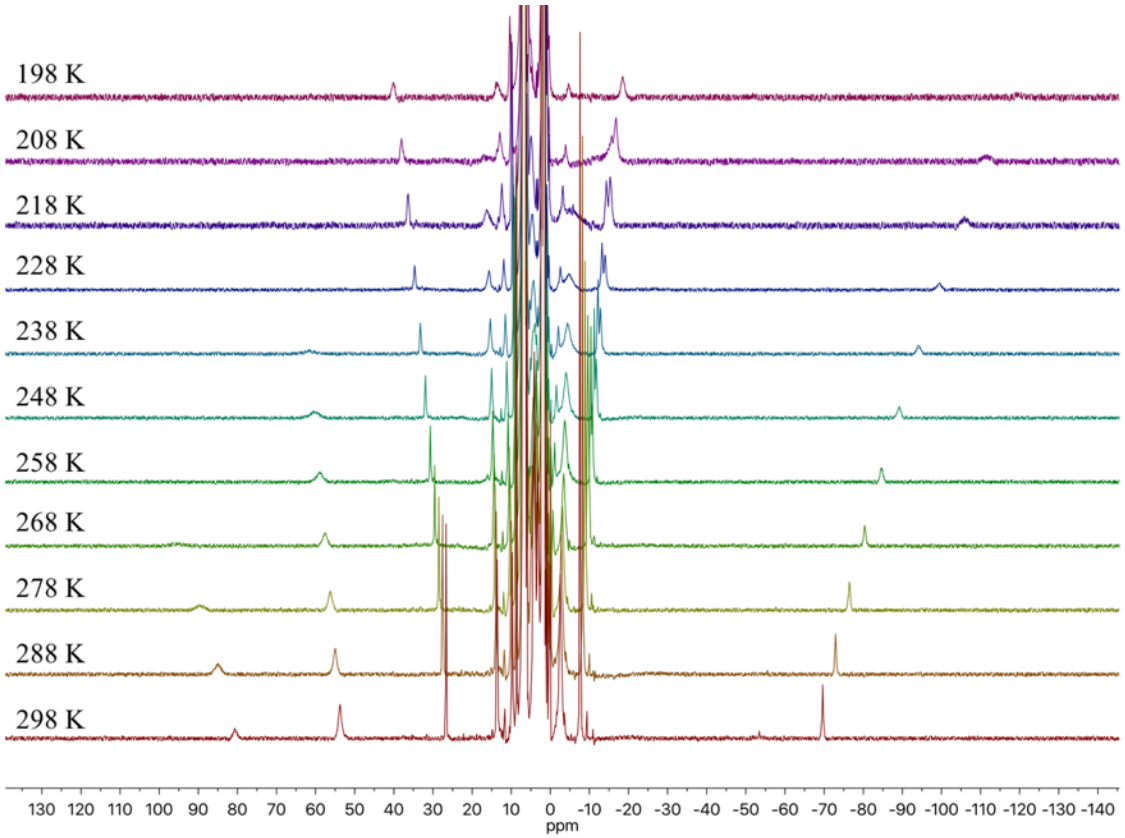


**Figure S55**. Variable temperature $^1H$ NMR spectra (500 MHz) of **6** in $C_6D_5CD_3$

| Temperature (K) | $\mu_{eff}/\mu_B$ |
|---|---|
| 298 | 4.79 |
| 288 | 4.82 |
| 278 | 4.83 |
| 268 | 4.86 |
| 258 | 4.88 |
| 248 | 4.90 |
| 238 | 4.93 |
| 228 | 4.95 |
| 218 | 4.98 |
| 208 | 5.00 |
| 198 | 5.02 |

**Table S1.** Solution state magnetic susceptibility of **6** in $C_6D_5CD_3$ at variable temperatures

*Time-course UV-Vis spectra*

* Note: For Tables S2 – S8, concentrations of **8-H** and **8-D** over time were obtained by fitting the 640 nm – 900 nm region of the corresponding time-course UV-vis traces following the conversion of **8-H** or **8-D** to **6**. The absorbance data (Abs) were fit to Gaussian lineshapes with the following equation:

$$Abs = a * e^{\left(-\left(\frac{\lambda-606.5}{b^2}\right)^2\right)} + c * e^{\left(-\left(\frac{\lambda-677.3}{d^2}\right)^2\right)} + f * e^{\left(-\left(\frac{\lambda-774.5}{g^2}\right)^2\right)} + \mathrm{h}$$

*Eyring plot analysis*

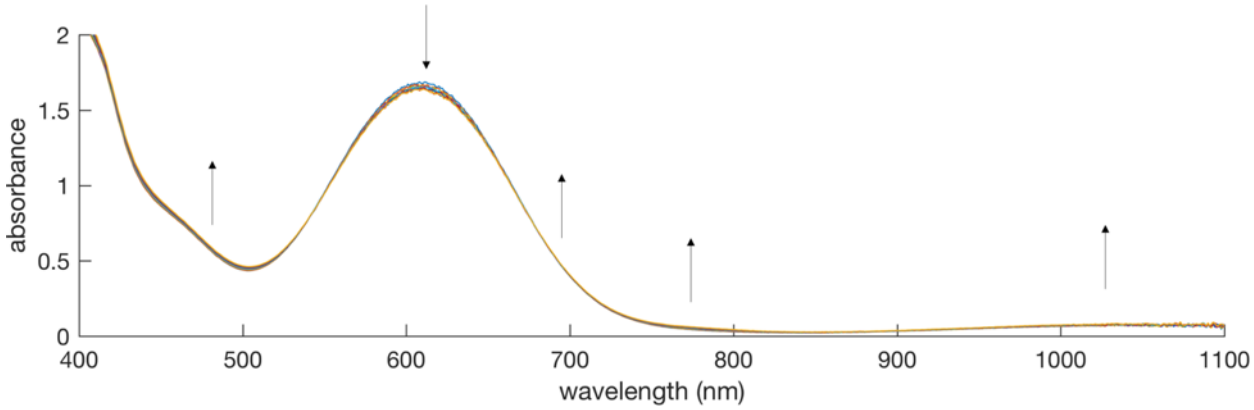


**Figure S56.** UV-visible spectra showing the conversion of **8-H** to **6** at 15 °C in a 1 mm cuvette; traces collected every 30 min for 270 min

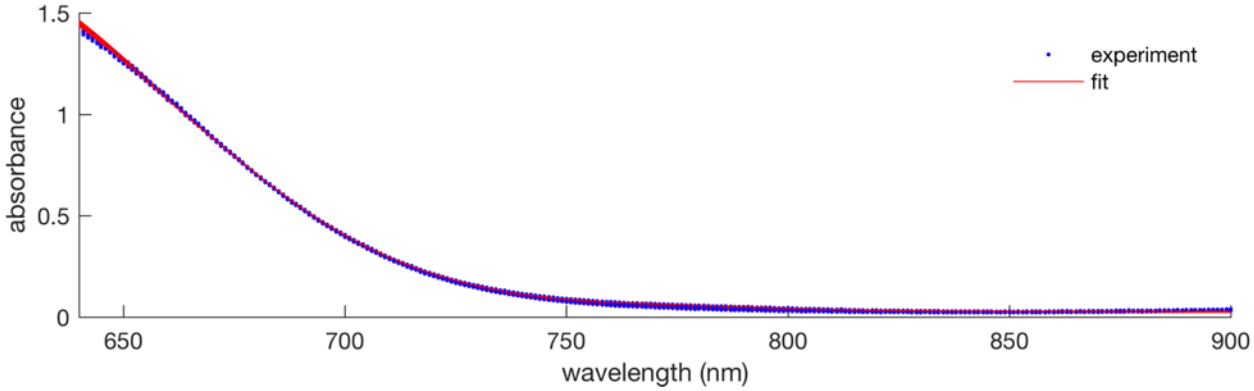


**Figure S57.** Partial UV-vis spectra and fits (640 nm to 900 nm region of Fig. S56)

| Time (min) | [8-H] (mol/L) |
|---|---|
| 0 | 0.006212 |
| 30 | 0.006191 |
| 60 | 0.006163 |
| 90 | 0.006148 |
| 120 | 0.006113 |
| 150 | 0.006081 |
| 180 | 0.006095 |
| 210 | 0.006078 |
| 240 | 0.006039 |
| 270 | 0.006049 |

**Table S2.** Fitted concentration of **8-H** vs. time (at 15 °C)

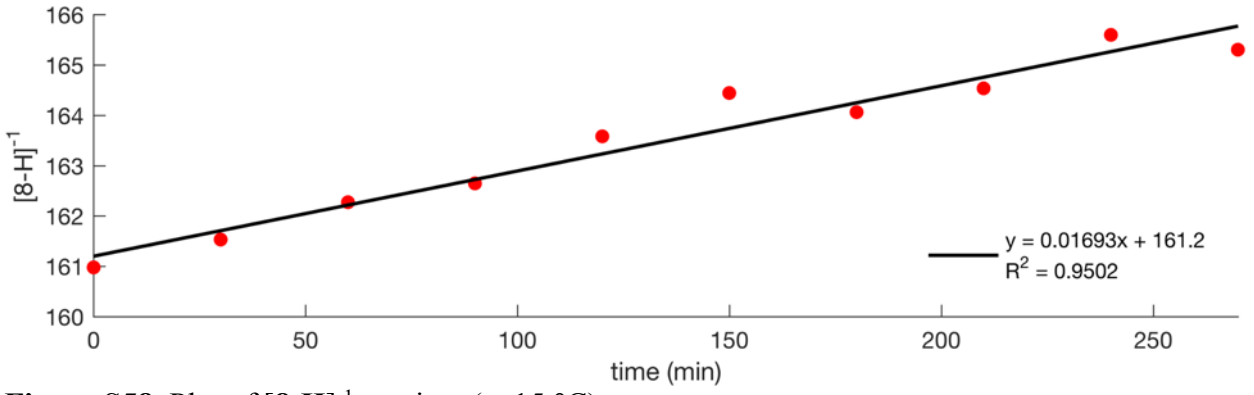


**Figure S58.** Plot of [**8-H**]$^{-1}$ vs. time (at 15 °C)

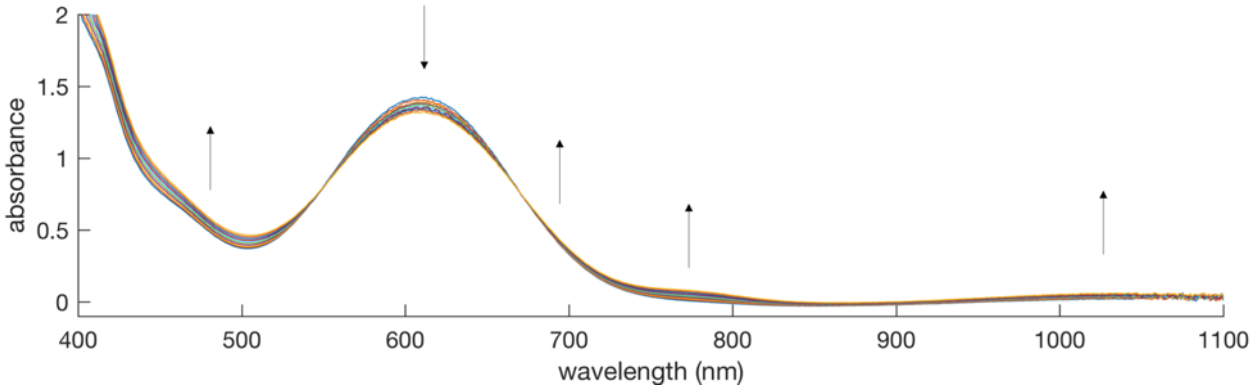


**Figure S59.** UV-visible spectra showing the conversion of **8-H** to **6** at 25 °C in a 1 mm cuvette; traces collected every 30 min for 270 min

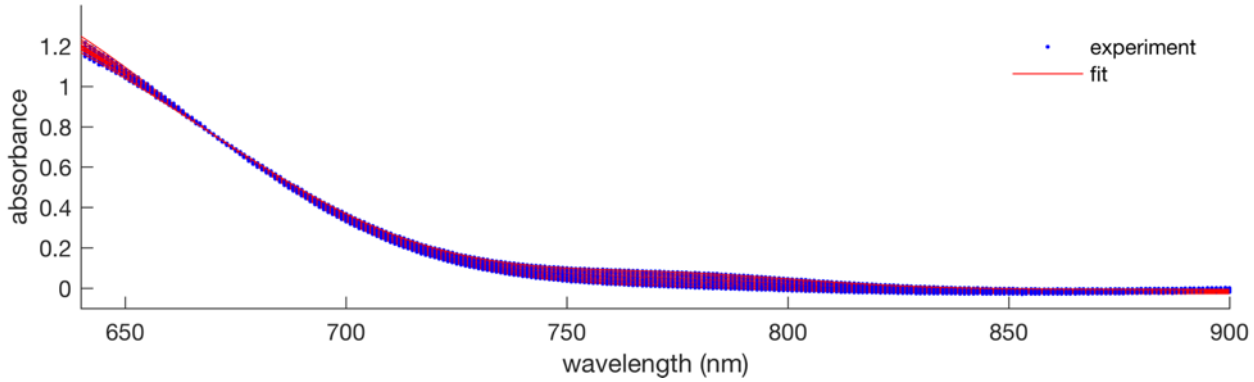


**Figure S60.** Partial UV-vis spectra and fits (640 nm to 900 nm region of Fig. S59)

| Time (min) | [8-H] (mol/L) |
|---|---|
| 0 | 0.005435 |
| 30 | 0.005346 |
| 60 | 0.005276 |
| 90 | 0.005261 |
| 120 | 0.005184 |
| 150 | 0.005144 |
| 180 | 0.005095 |
| 210 | 0.005032 |
| 240 | 0.004993 |
| 270 | 0.004908 |

**Table S3.** Fitted concentration of **8-H** vs. time (at 25 °C)

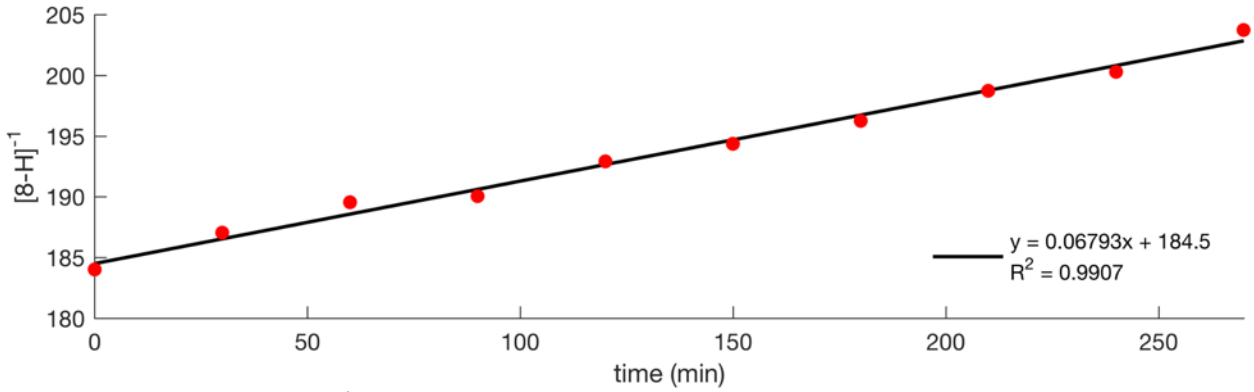


**Figure S61.** Plot of [**8-H**]$^{-1}$ vs time (at 25 °C)

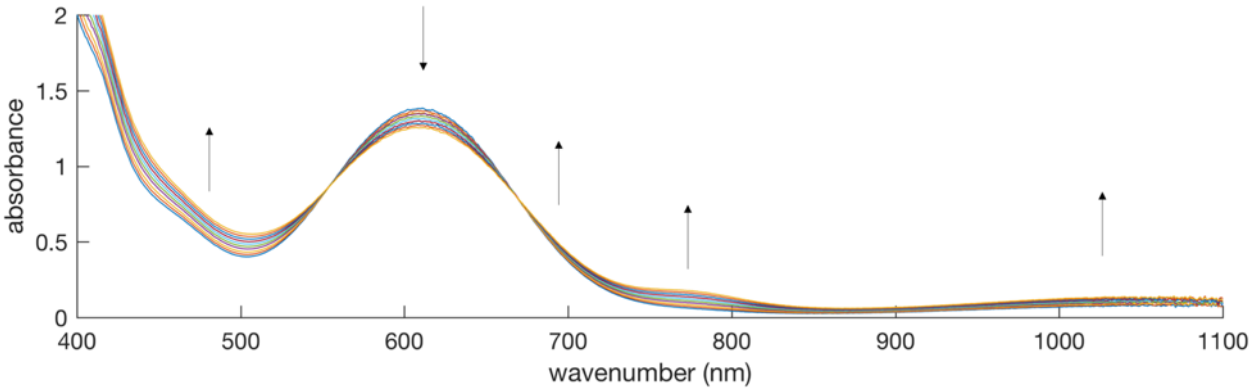


**Figure S62.** UV-visible spectra showing the conversion of **8-H** to **6** at 30 °C in a 1 mm cuvette; traces collected every 30 min for 270 min

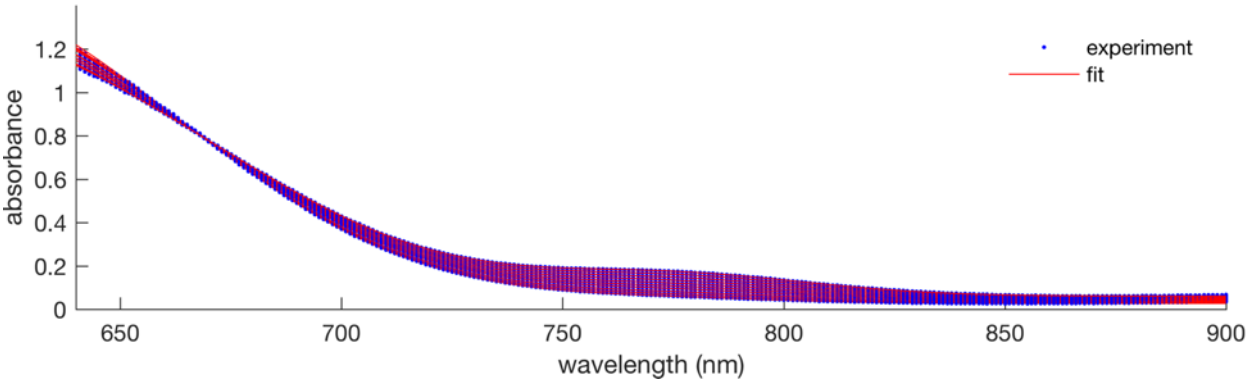


**Figure S63.** Partial UV-vis spectra and fits (640 nm to 900 nm region of Fig. S62)

| Time (min) | [8-H] (mol/L) |
|---|---|
| 0 | 0.005067 |
| 30 | 0.004989 |
| 60 | 0.004936 |
| 90 | 0.004869 |
| 120 | 0.004756 |
| 150 | 0.004721 |
| 180 | 0.004625 |
| 210 | 0.004551 |
| 240 | 0.004449 |
| 270 | 0.004389 |

**Table S4.** Fitted concentration of **8-H** vs. time (at 30 °C)

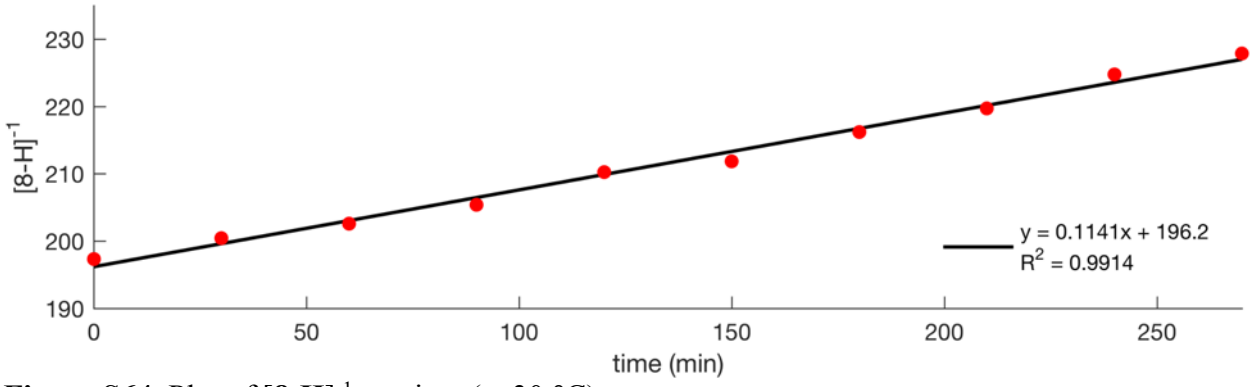


**Figure S64.** Plot of [**8-H**]$^{-1}$ vs. time (at 30 °C)

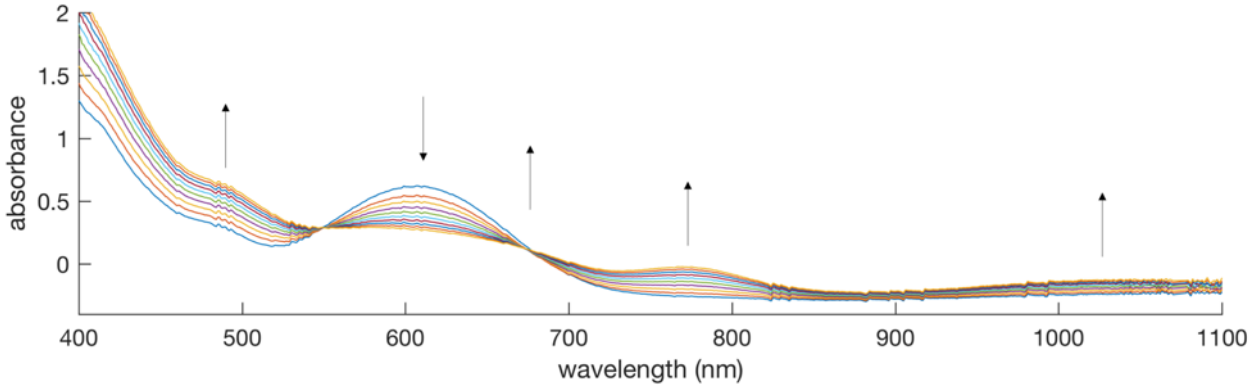


**Figure S65.** UV-visible spectra showing the conversion of **8-H** to **6** at 40 °C in a 1 mm cuvette; traces collected every 30 min for 270 min

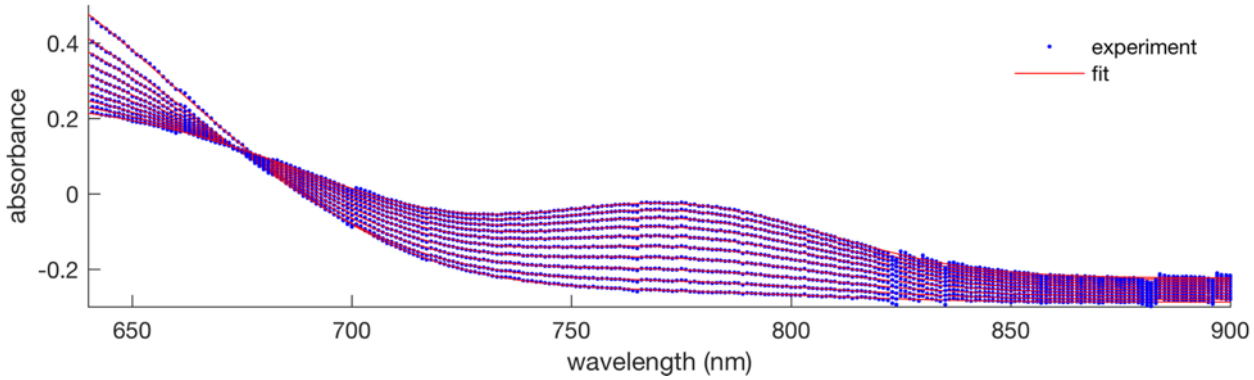


**Figure S66.** Partial UV-vis spectra and fits (640 nm to 900 nm region of Fig. S65)

| Time (min) | [8-H] (mol/L) |
|---|---|
| 0 | 0.003282 |
| 30 | 0.002946 |
| 60 | 0.002723 |
| 90 | 0.002510 |
| 120 | 0.002307 |
| 150 | 0.002124 |
| 180 | 0.001949 |
| 210 | 0.001806 |
| 240 | 0.001668 |
| 270 | 0.001547 |

**Table S5.** Fitted concentration of **8-H** vs. time (at 40 °C)

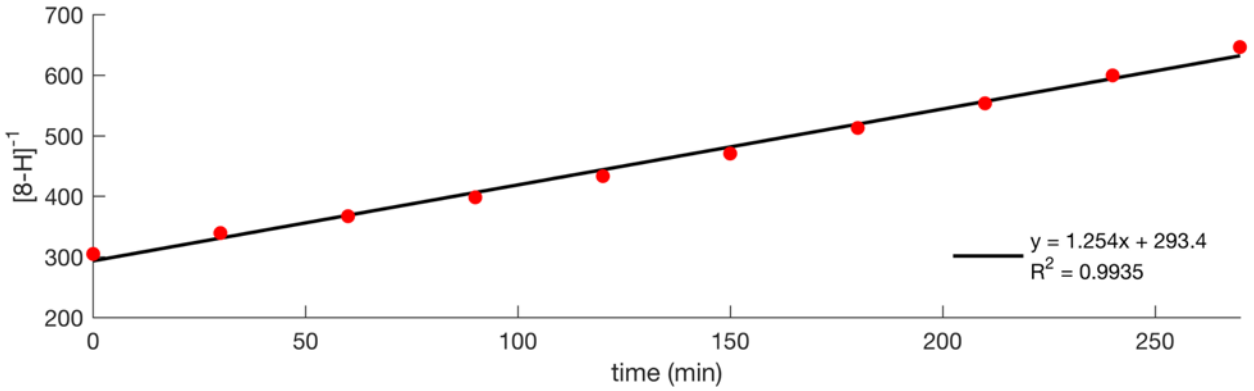


**Figure S67.** Plot of [**8-H**]$^{-1}$ vs. time (at 40 °C)

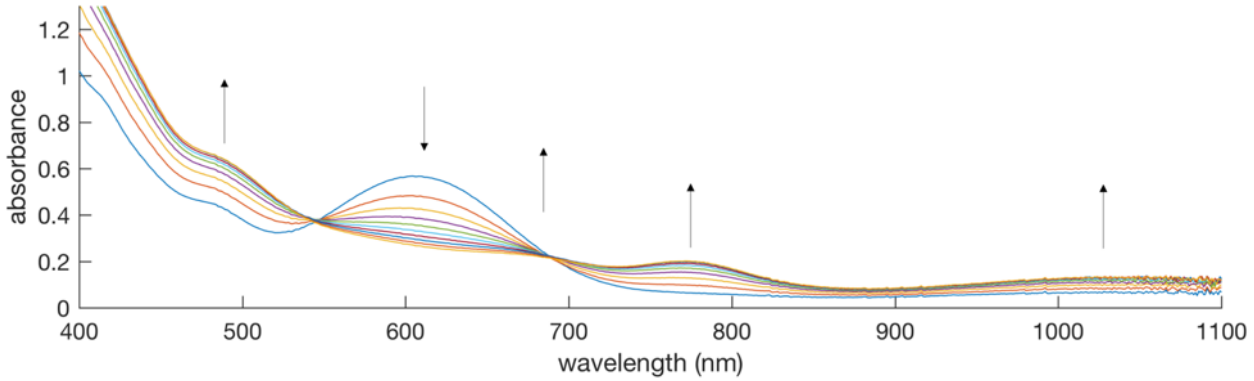


**Figure S68.** UV-visible spectra showing the conversion of **8-H** to **6** at 50 °C in a 1 mm cuvette; traces collected every 30 min for 270 min

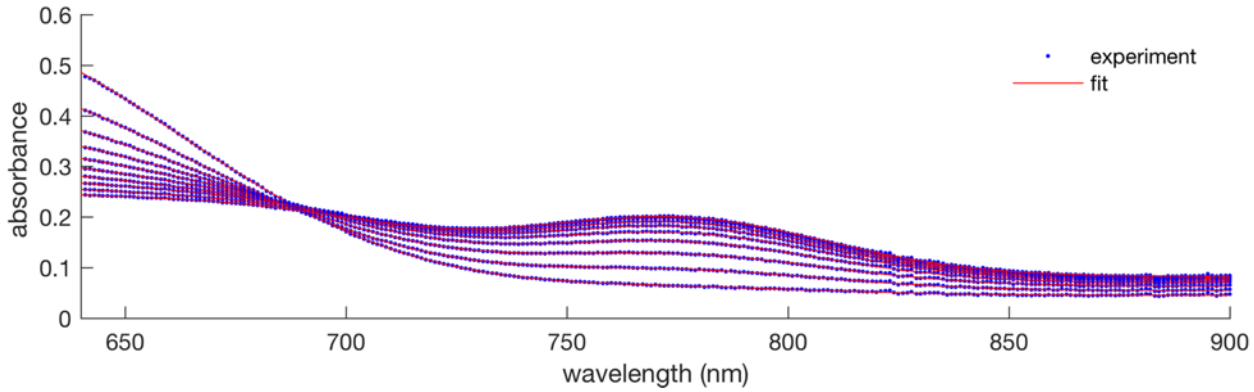


**Figure S69.** Partial UV-vis spectra and fits (640 nm to 900 nm region of Fig. S68)

| Time (min) | [8-H] (mol/L) |
|---|---|
| 0 | 0.001873 |
| 30 | 0.001438 |
| 60 | 0.001155 |
| 90 | 0.0009611 |
| 120 | 0.0008223 |
| 150 | 0.0007216 |
| 180 | 0.0006399 |
| 210 | 0.0005678 |
| 240 | 0.0005187 |
| 270 | 0.0004784 |

**Table S6.** Fitted concentration of **8-H** vs. time (at 50 °C)

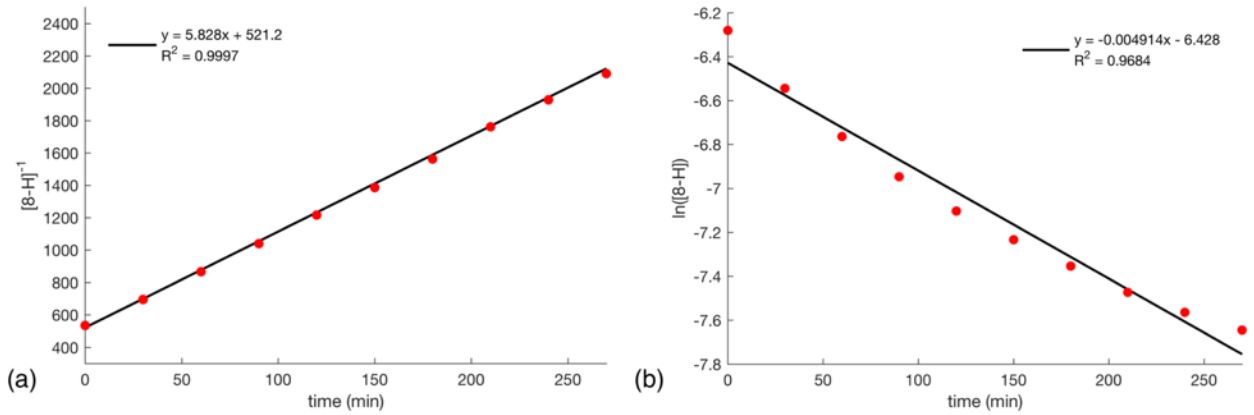


**Figure S70.** (a) Plot of [**8-H**]$^{-1}$ vs. time (at 50 °C) (b) Plot of ln([**8-H**]) vs. time (at 50 °C)

| T (K) | k ($M^{-1}$3$min^{-1}$ ) |
|---|---|
| 288 | 0.01693 |
| 298 | 0.06793 |
| 303 | 0.1141 |
| 313 | 1.254 |
| 323 | 5.828 |

**Table S7.** Temperature dependence of the second order rate constant (k) for the conversion of **8-H** to **6**

*Kinetic isotope effect*

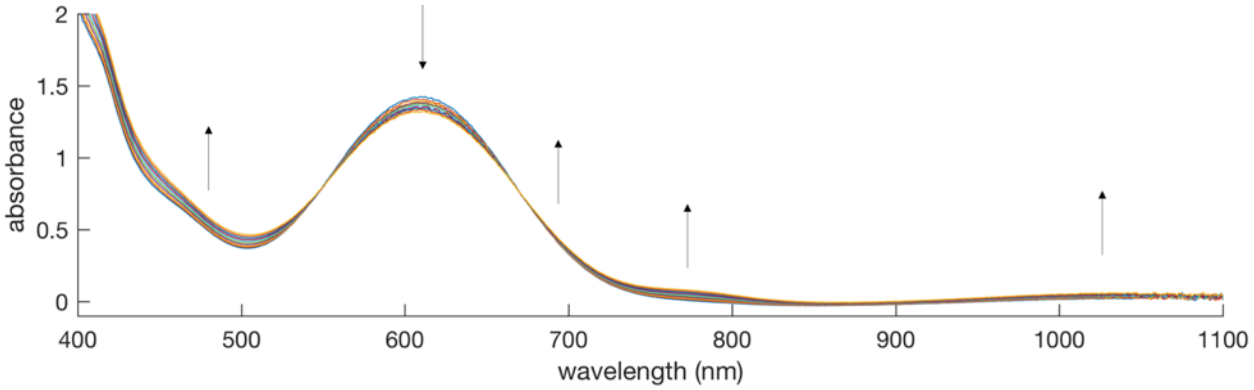


**Figure S71.** UV-visible spectra showing the conversion of **8-D** to **6** at 25 °C in a 1 mm cuvette; traces collected every 30 min for 270 min

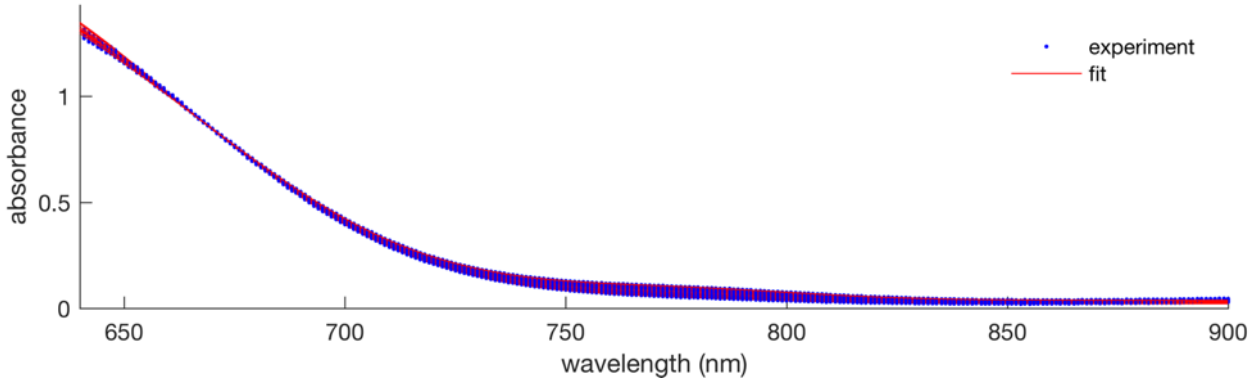


**Figure S72.** Partial UV-vis spectra and fits (640 nm to 900 nm region of Fig. S71)

| Time (min) | [8-D] (mol/L) |
|---|---|
| 0 | 0.005650 |
| 30 | 0.005604 |
| 60 | 0.005534 |
| 90 | 0.005523 |
| 120 | 0.005466 |
| 150 | 0.005452 |
| 180 | 0.005420 |
| 210 | 0.005371 |
| 240 | 0.005378 |
| 270 | 0.005304 |

**Table S8.** Fitted concentration of **8-D** vs. time (at 25 °C)

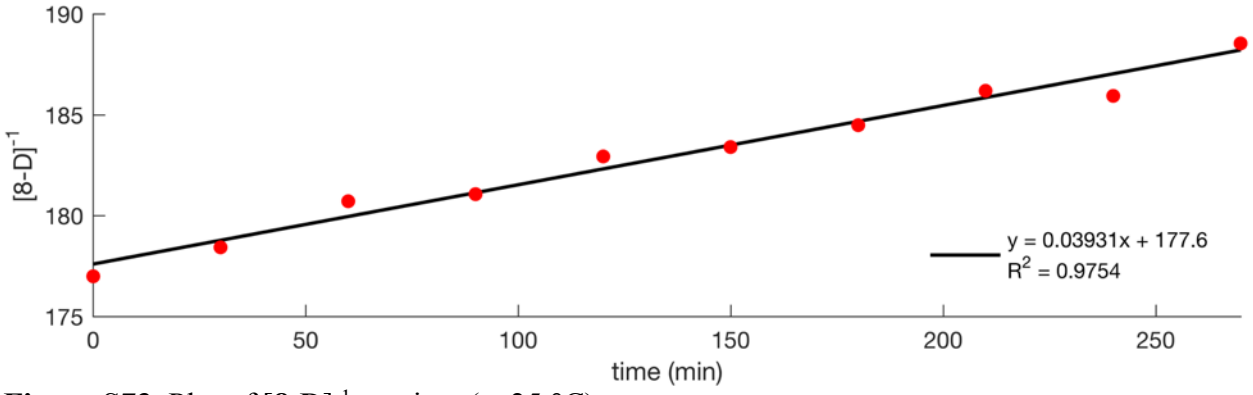


**Figure S73.** Plot of [**8-D**]$^{-1}$ vs. time (at 25 °C)

*DFT-optimized structures*

| | | | |
|---|---|---|---|
| Fe | 0.51351100 | 0.05922200 | -1.03017400 |
| P | 1.38765300 | -1.99402600 | -0.80215900 |
| S | -1.71508100 | -0.14263000 | -0.79525400 |
| P | 1.05446900 | 2.21884800 | -0.77401200 |
| Si | 0.60659500 | 0.05068200 | 1.24023200 |
| N | 0.23385300 | 0.04219400 | -2.87573300 |
| C | 2.05136100 | -2.32109200 | 0.87337700 |
| C | 2.78554100 | -2.48360700 | -1.93306000 |
| H | 2.97617200 | -3.54564700 | -1.69634900 |
| C | 1.55693400 | 2.65748400 | 0.93360400 |
| C | -3.53858000 | -0.17437400 | 1.30077700 |
| C | 1.36786000 | 1.66557100 | 1.90902300 |
| C | -3.84306400 | -0.21410100 | 2.66995700 |
| H | -4.89541600 | -0.26191500 | 2.96501000 |
| C | 0.11806900 | -3.36551600 | -1.02362700 |
| H | -0.51582500 | -2.98556600 | -1.84531000 |
| C | 2.77406700 | -2.81946800 | 3.51871600 |
| H | 3.05124800 | -3.01623200 | 4.55755400 |
| C | -0.30566400 | 3.47812400 | -1.07459500 |
| H | 0.22290800 | 4.45108700 | -1.08557200 |
| C | 2.84490100 | -3.43330100 | 1.18651200 |
| H | 3.19218400 | -4.11215100 | 0.40128600 |
| C | -2.85275700 | -0.16608500 | 3.64651400 |
| H | -3.12464200 | -0.18637200 | 4.70452400 |
| C | 2.48741800 | 2.85356900 | -1.80672600 |
| H | 2.36561000 | 3.95292700 | -1.82998500 |
| C | 1.62901900 | -1.42952600 | 1.87731700 |
| C | 1.99659600 | -1.70670700 | 3.20315600 |
| H | 1.67318400 | -1.04463400 | 4.01268300 |
| C | 4.05687000 | -1.70046500 | -1.65359400 |
| H | 3.93062700 | -0.63702500 | -1.90748400 |
| H | 4.88497600 | -2.08449300 | -2.26822500 |
| H | 4.37011600 | -1.75606000 | -0.60123600 |
| C | -1.16237000 | -0.05528300 | 1.90623700 |
| C | 3.20822400 | -3.67884100 | 2.50817600 |
| H | 3.82949400 | -4.54395500 | 2.75247100 |
| C | -0.73885000 | -3.47953500 | 0.22907700 |
| H | -0.18654400 | -3.97226800 | 1.04407300 |
| H | -1.63524300 | -4.08295800 | 0.02412500 |
| H | -1.08282200 | -2.50551900 | 0.60168200 |
| C | -4.65929900 | -0.23083700 | 0.33392800 |
| C | -2.17354400 | -0.10392800 | 0.92144800 |
| C | 2.45502100 | 2.32318900 | -3.23196300 |
| H | 2.65142000 | 1.23972900 | -3.24509100 |

| | | | |
|---|---|---|---|
| H | 3.24098200 | 2.80395300 | -3.83320700 |
| H | 1.50057700 | 2.48751600 | -3.74801800 |
| C | 2.15245900 | 3.24455600 | 3.58925200 |
| H | 2.38630000 | 3.47308900 | 4.63223100 |
| C | -1.51664900 | -0.08320000 | 3.25849300 |
| H | -0.73717300 | -0.04194900 | 4.02778900 |
| C | -1.00032000 | 3.27047600 | -2.41066500 |
| H | -0.31240400 | 3.27797500 | -3.26697400 |
| H | -1.73923200 | 4.06768700 | -2.58186300 |
| H | -1.54409600 | 2.31322400 | -2.42192500 |
| C | 2.02809900 | 3.93142100 | 1.27978800 |
| H | 2.16433100 | 4.70249600 | 0.51341700 |
| C | 2.32828200 | 4.22286400 | 2.60674500 |
| H | 2.69796200 | 5.21439500 | 2.87960500 |
| C | 3.82638600 | 2.51682000 | -1.16533800 |
| H | 3.98919000 | 3.02134800 | -0.20500400 |
| H | 4.65018200 | 2.80212500 | -1.83666100 |
| H | 3.91600300 | 1.43393900 | -0.98370400 |
| N | -0.02147200 | 0.03228300 | -3.97141000 |
| C | 1.67558800 | 1.98339200 | 3.24210000 |
| H | 1.53661500 | 1.23760000 | 4.03101000 |
| C | -1.31272000 | 3.47638800 | 0.06507100 |
| H | -1.79419400 | 2.49251900 | 0.16744000 |
| H | -2.10912700 | 4.20922700 | -0.13456200 |
| H | -0.86441800 | 3.73111400 | 1.03483900 |
| C | -5.64232600 | -1.22308900 | 0.46891100 |
| H | -5.53639300 | -1.96953000 | 1.26156600 |
| C | -6.72900300 | -1.28274300 | -0.40071800 |
| H | -7.47562300 | -2.07215600 | -0.28312600 |
| C | -4.80826900 | 0.71348600 | -0.69423700 |
| H | -4.06361800 | 1.50530400 | -0.80583700 |
| C | -6.86083300 | -0.34068300 | -1.41911400 |
| H | -7.71225400 | -0.38357300 | -2.10267500 |
| C | 2.38522300 | -2.37470400 | -3.39645400 |
| H | 1.40738300 | -2.82686100 | -3.61844500 |
| H | 3.12964400 | -2.86749000 | -4.03945200 |
| H | 2.33389700 | -1.32286600 | -3.71089300 |
| C | -5.89834300 | 0.65998000 | -1.55803600 |
| H | -5.99937200 | 1.40955400 | -2.34681400 |
| C | 0.68229100 | -4.72295200 | -1.41064000 |
| H | 1.21633300 | -4.72330000 | -2.37056600 |
| H | -0.13729300 | -5.45202600 | -1.50030600 |
| H | 1.36501100 | -5.11500800 | -0.64046200 |
| H | 2.05682000 | 0.17816000 | -1.08009400 |

**Table S9.** Gas-phase optimized coordinates for **8-H** (m06l, $S = 1/2$)

| | | | |
|---|---|---|---|
| Fe | -0.40651200 | -0.02742200 | -1.05973600 |
| P | -1.43431500 | -1.97339400 | -0.67790500 |
| P | -1.47887300 | 1.90612200 | -0.82623600 |
| S | 1.88980900 | 0.04304100 | -0.87360400 |
| Si | -0.38392000 | 0.06386500 | 1.20164500 |
| C | -0.20460800 | -3.40847500 | -0.91118300 |
| H | -0.82326500 | -4.32563600 | -0.98560600 |
| N | -0.37449700 | -0.10237400 | -2.88106500 |
| C | -0.46129900 | 3.39985700 | -1.40816200 |
| H | -1.15610800 | 4.26289800 | -1.40683700 |
| N | -0.34305500 | -0.15563500 | -4.01698500 |
| C | -1.77546700 | 2.46941900 | 0.90585200 |
| C | -1.20236000 | 1.65625700 | 1.89688700 |
| C | 1.40432300 | 0.02232900 | 1.84428300 |
| C | 2.39150100 | 0.05601300 | 0.82501400 |
| C | -1.92292100 | -2.27864500 | 1.08060000 |
| C | 3.76805300 | 0.03633800 | 1.18984800 |
| C | -2.41834300 | 3.66788700 | 1.24311000 |
| H | -2.85458700 | 4.30070700 | 0.46096600 |
| C | 4.88003000 | 0.02388600 | 0.21155200 |
| C | 0.68241700 | 3.68080300 | -0.44340800 |
| H | 0.33745000 | 3.98733100 | 0.55378800 |
| H | 1.32541600 | 4.48606000 | -0.83464100 |
| H | 1.31482700 | 2.78660600 | -0.31997200 |
| C | -1.63166400 | -1.57200000 | 3.36991500 |
| H | -1.22545300 | -0.87423400 | 4.11080000 |
| C | -1.28145900 | 2.08441000 | 3.23205100 |
| H | -0.82541600 | 1.48435300 | 4.02775900 |
| C | -1.92284300 | 3.27472800 | 3.57152700 |
| H | -1.97466300 | 3.59124400 | 4.61779100 |
| C | 4.97186900 | 0.93932000 | -0.85099900 |
| H | 4.17406400 | 1.67164500 | -0.98880900 |
| C | -1.38294800 | -1.36453300 | 2.00478000 |
| C | 0.61512300 | -3.23876400 | -2.18322000 |
| H | 0.01057600 | -3.05712400 | -3.08128200 |
| H | 1.22831200 | -4.13588800 | -2.36818700 |
| H | 1.30000400 | -2.38292900 | -2.08216900 |
| C | -2.93231700 | -3.54707000 | 2.88429900 |
| H | -3.53643500 | -4.39388600 | 3.22351500 |
| C | 3.13831800 | -0.05071400 | 3.55221800 |
| H | 3.43334400 | -0.08706100 | 4.60456300 |
| C | 0.72764900 | -3.53665100 | 0.28488800 |
| H | 1.27143300 | -2.59352600 | 0.46132100 |
| H | 1.48800000 | -4.31183900 | 0.09728100 |
| H | 0.20237800 | -3.80037900 | 1.21349600 |

| | | | |
|---|---|---|---|
| C | -2.68935900 | -3.36522500 | 1.52363200 |
| H | -3.09876900 | -4.08675400 | 0.80871000 |
| C | 1.79201600 | -0.03185500 | 3.18508200 |
| H | 1.02628800 | -0.06885400 | 3.96959100 |
| C | 6.06222700 | 0.92220400 | -1.71662100 |
| H | 6.11239700 | 1.64892400 | -2.53235600 |
| C | -2.39968400 | -2.64898900 | 3.81117000 |
| H | -2.58801600 | -2.78979100 | 4.87994400 |
| C | 7.08467900 | -0.01488500 | -1.55471700 |
| H | 7.93295100 | -0.03152000 | -2.24468100 |
| C | -2.92928000 | -2.71066000 | -1.57385100 |
| H | -3.03334800 | -3.74105200 | -1.18475600 |
| C | -3.15962400 | 2.26070500 | -1.62529700 |
| H | -3.25088500 | 3.35734400 | -1.74795600 |
| C | 0.08380600 | 3.19219700 | -2.81132100 |
| H | 0.79248600 | 2.34982400 | -2.82368600 |
| H | 0.62894100 | 4.08749900 | -3.15232600 |
| H | -0.69455800 | 2.97953000 | -3.55771400 |
| C | -2.49820000 | 4.06776000 | 2.57505600 |
| H | -3.00208800 | 5.00238600 | 2.83929300 |
| C | 4.10482600 | -0.02007600 | 2.55165500 |
| H | 5.16589100 | -0.02370000 | 2.82258100 |
| C | 7.00905700 | -0.93065300 | -0.50730100 |
| H | 7.79729600 | -1.67679100 | -0.37138200 |
| C | -4.19967100 | -1.94277800 | -1.25194400 |
| H | -4.35214000 | -1.80022500 | -0.17176300 |
| H | -5.08474400 | -2.46755200 | -1.64753200 |
| H | -4.18235400 | -0.94588400 | -1.71620800 |
| C | 5.92196100 | -0.90558100 | 0.36415000 |
| H | 5.85817200 | -1.63705400 | 1.17522900 |
| C | -4.28078800 | 1.76207300 | -0.72221400 |
| H | -4.05218400 | 0.75977200 | -0.32437700 |
| H | -5.23272600 | 1.68697100 | -1.27330600 |
| H | -4.44543700 | 2.41369700 | 0.14567300 |
| C | -3.23584400 | 1.60036100 | -2.99251800 |
| H | -2.46586400 | 1.95801000 | -3.68904100 |
| H | -4.21850600 | 1.77078400 | -3.46235600 |
| H | -3.08691400 | 0.51254000 | -2.90119400 |
| C | -2.72991600 | -2.79457000 | -3.07860200 |
| H | -2.47058600 | -1.81481600 | -3.50887900 |
| H | -3.65538100 | -3.13391500 | -3.57273400 |
| H | -1.93743900 | -3.49890300 | -3.36360100 |

**Table S10**. Gas-phase optimized coordinates for **9** (m06l, $S = 1/2$)

| | | | |
|---|---|---|---|
| Fe | 0.51937400 | 0.06404600 | -1.02451700 |
| P | 1.40648300 | -1.99850900 | -0.80591400 |
| S | -1.72736800 | -0.12756600 | -0.82249300 |
| P | 1.08641900 | 2.23212000 | -0.75962900 |
| Si | 0.58462200 | 0.04165800 | 1.24653400 |
| N | 0.29356300 | 0.06672600 | -2.86412100 |
| C | 2.03901100 | -2.32546600 | 0.88245900 |
| C | 2.82252300 | -2.46267100 | -1.91736700 |
| H | 3.01923300 | -3.52234200 | -1.67811100 |
| C | 1.52205600 | 2.65825300 | 0.96963700 |
| C | -3.57213700 | -0.18872400 | 1.26456400 |
| C | 1.31530100 | 1.66053700 | 1.93700800 |
| C | -3.88555500 | -0.25027300 | 2.63248700 |
| H | -4.93888300 | -0.30721500 | 2.92313200 |
| C | 0.14401300 | -3.36863200 | -1.05790500 |
| H | -0.47076300 | -2.98954900 | -1.89417600 |
| C | 2.73318700 | -2.83190900 | 3.53558600 |
| H | 3.00009600 | -3.03224400 | 4.57668900 |
| C | -0.24681600 | 3.49911300 | -1.11844400 |
| H | 0.29569400 | 4.46262000 | -1.10649700 |
| C | 2.83365400 | -3.43662700 | 1.19908800 |
| H | 3.19028000 | -4.11042500 | 0.41413600 |
| C | -2.90099600 | -0.21684300 | 3.61627900 |
| H | -3.17904500 | -0.25538800 | 4.67249800 |
| C | 2.57523000 | 2.82990800 | -1.72661700 |
| H | 2.47838900 | 3.93079900 | -1.74358400 |
| C | 1.60093100 | -1.44006000 | 1.88677400 |
| C | 1.95465900 | -1.71916300 | 3.21748700 |
| H | 1.62092200 | -1.06005700 | 4.02519000 |
| C | 4.07968000 | -1.66666400 | -1.61764300 |
| H | 3.95737200 | -0.60699400 | -1.88982100 |
| H | 4.92328700 | -2.05551400 | -2.20797800 |
| H | 4.37437400 | -1.70802000 | -0.55865200 |
| C | -1.19936900 | -0.07745100 | 1.88507800 |
| C | 3.18135400 | -3.68579000 | 2.52527300 |
| H | 3.80243300 | -4.55041600 | 2.77281500 |
| C | -0.73588000 | -3.49058900 | 0.17665000 |
| H | -0.20223300 | -3.99560700 | 0.99710300 |
| H | -1.63053500 | -4.09102400 | -0.04786300 |
| H | -1.08167200 | -2.51733100 | 0.55303500 |
| C | -4.69242100 | -0.23425200 | 0.29448400 |
| C | -2.20417500 | -0.11158200 | 0.89060800 |
| C | 2.59326300 | 2.31065100 | -3.15567900 |
| H | 2.76570900 | 1.22278000 | -3.17784000 |
| H | 3.41942500 | 2.77862700 | -3.71195300 |
| H | 1.67049100 | 2.51326300 | -3.71498400 |

| | | | |
|---|---|---|---|
| C | 2.05300700 | 3.23545100 | 3.64266000 |
| H | 2.26200400 | 3.46068000 | 4.69192200 |
| C | -1.56173800 | -0.12764000 | 3.23581800 |
| H | -0.78558200 | -0.10146000 | 4.00924900 |
| C | -0.88357100 | 3.30405000 | -2.48387200 |
| H | -0.15554900 | 3.30972200 | -3.30618500 |
| H | -1.60285300 | 4.11297100 | -2.68327400 |
| H | -1.44064300 | 2.35496700 | -2.53042600 |
| C | 1.98000600 | 3.93341700 | 1.33176400 |
| H | 2.12955400 | 4.70631300 | 0.57032800 |
| C | 2.24688100 | 4.21911800 | 2.66774000 |
| H | 2.60539100 | 5.21131000 | 2.95386800 |
| C | 3.87436300 | 2.45749300 | -1.02778000 |
| H | 4.01796300 | 2.97444000 | -0.07024500 |
| H | 4.73106400 | 2.71241000 | -1.66974400 |
| H | 3.93091500 | 1.37414100 | -0.83189000 |
| N | 0.06687200 | 0.07061500 | -3.96813400 |
| C | 1.58959100 | 1.97219100 | 3.28048900 |
| H | 1.43580400 | 1.22214200 | 4.06266300 |
| C | -1.30227100 | 3.51381600 | -0.02473900 |
| H | -1.79760900 | 2.53495900 | 0.06795500 |
| H | -2.08393000 | 4.25010100 | -0.26763600 |
| H | -0.89661800 | 3.78160600 | 0.96097000 |
| C | -5.67738000 | -1.22778400 | 0.41965400 |
| H | -5.57603600 | -1.98302700 | 1.20472000 |
| C | -6.76654900 | -1.27592200 | -0.44934300 |
| H | -7.51416800 | -2.06563900 | -0.33842300 |
| C | -4.84408400 | 0.72410900 | -0.72217700 |
| H | -4.10233400 | 1.52046500 | -0.82396300 |
| C | -6.90059200 | -0.32083500 | -1.45656700 |
| H | -7.75396600 | -0.35434700 | -2.13861300 |
| C | 2.44256900 | -2.35217600 | -3.38579700 |
| H | 1.46284900 | -2.79400500 | -3.62077500 |
| H | 3.19053800 | -2.85981500 | -4.01316200 |
| H | 2.41634900 | -1.30052600 | -3.70627700 |
| C | -5.93717700 | 0.68209700 | -1.58495700 |
| H | -6.04095700 | 1.44369000 | -2.36224400 |
| C | 0.72193800 | -4.72021600 | -1.44186400 |
| H | 1.26952600 | -4.71017700 | -2.39385200 |
| H | -0.09510900 | -5.45022600 | -1.55000600 |
| H | 1.39668600 | -5.11421100 | -0.66602300 |
| H | 2.05996600 | 0.17104800 | -1.02231200 |

**Table S11**. Optimized coordinates for **8-H** with MeCN solvation (m06l, $S = 1/2$)

| | | | |
|---|---|---|---|
| Fe | 0.48346400 | 0.07403100 | -1.09971000 |
| P | 1.50080400 | -2.00381700 | -0.79711900 |
| S | -1.81017900 | -0.07945800 | -0.87777700 |
| P | 1.16000500 | 2.27375100 | -0.74716800 |
| Si | 0.52214500 | 0.04646900 | 1.20664600 |
| N | 0.27529700 | 0.06980100 | -2.94778000 |
| C | 2.06720800 | -2.29739500 | 0.91979100 |
| C | 2.95866200 | -2.45705200 | -1.85947200 |
| H | 3.18043600 | -3.51200200 | -1.61962000 |
| C | 1.45179800 | 2.69435600 | 1.01100000 |
| C | -3.64523100 | -0.22657600 | 1.21944000 |
| C | 1.18688400 | 1.67952500 | 1.94703300 |
| C | -3.94651600 | -0.33448500 | 2.58734100 |
| H | -4.99691800 | -0.40996600 | 2.88474300 |
| C | 0.25167300 | -3.37583200 | -1.07887400 |
| H | -0.33053100 | -3.01741500 | -1.94718600 |
| C | 2.67802600 | -2.73017400 | 3.60592800 |
| H | 2.91382800 | -2.89942900 | 4.66005100 |
| C | -0.04946100 | 3.59810000 | -1.26887100 |
| H | 0.53401300 | 4.53670200 | -1.23251000 |
| C | 2.87663000 | -3.38144100 | 1.28915000 |
| H | 3.27516700 | -4.06241400 | 0.53088800 |
| C | -2.95478600 | -0.32682000 | 3.56428600 |
| H | -3.22352600 | -0.40213200 | 4.62101200 |
| C | 2.78016000 | 2.70850000 | -1.57882500 |
| H | 2.78941000 | 3.81008400 | -1.66826300 |
| C | 1.56697000 | -1.40345500 | 1.88830500 |
| C | 1.88085700 | -1.64706300 | 3.23616300 |
| H | 1.50300900 | -0.98076000 | 4.01812300 |
| C | 4.17462100 | -1.61439900 | -1.51940800 |
| H | 3.98913600 | -0.54959500 | -1.72879700 |
| H | 5.03617300 | -1.91910100 | -2.13272400 |
| H | 4.47578700 | -1.70043300 | -0.46521500 |
| C | -1.26903100 | -0.11779300 | 1.82338700 |
| C | 3.18387700 | -3.59370500 | 2.63155400 |
| H | 3.81777500 | -4.43617200 | 2.91971200 |
| C | -0.67855000 | -3.47213500 | 0.12065700 |
| H | -0.17597700 | -3.94628100 | 0.97838800 |
| H | -1.55705500 | -4.08840000 | -0.12344200 |
| H | -1.04756800 | -2.48970100 | 0.44962600 |
| C | -4.77451500 | -0.26309700 | 0.25892200 |
| C | -2.28072700 | -0.12316700 | 0.83355600 |
| C | 2.87587300 | 2.09178700 | -2.96573500 |
| H | 2.90845300 | 0.99182100 | -2.90767700 |
| H | 3.80095800 | 2.41956500 | -3.46361200 |
| H | 2.03811500 | 2.35809300 | -3.62369200 |

| | | | |
|---|---|---|---|
| C | 1.82175800 | 3.22868200 | 3.71868600 |
| H | 1.96571100 | 3.43685200 | 4.78239700 |
| C | -1.61961700 | -0.21650200 | 3.17482000 |
| H | -0.83707000 | -0.21167900 | 3.94262600 |
| C | -0.56482900 | 3.38388100 | -2.68204800 |
| H | 0.23546900 | 3.31512700 | -3.43153200 |
| H | -1.21386900 | 4.22206600 | -2.97749700 |
| H | -1.16955200 | 2.46556400 | -2.74624500 |
| C | 1.89111600 | 3.96188000 | 1.41975900 |
| H | 2.08951800 | 4.74421300 | 0.67932000 |
| C | 2.07859500 | 4.22651400 | 2.77317600 |
| H | 2.42403800 | 5.21205100 | 3.09608300 |
| C | 3.95284400 | 2.26561400 | -0.71449100 |
| H | 4.05041700 | 2.85575200 | 0.20603500 |
| H | 4.89655300 | 2.36561100 | -1.27198600 |
| H | 3.86369000 | 1.20759300 | -0.41674300 |
| N | 0.08540600 | 0.06395900 | -4.06118800 |
| C | 1.37758700 | 1.97265700 | 3.30955300 |
| H | 1.17325500 | 1.21293400 | 4.07094000 |
| C | -1.20540700 | 3.69250900 | -0.28412000 |
| H | -1.75678200 | 2.74031400 | -0.22444200 |
| H | -1.91830200 | 4.46311900 | -0.61477100 |
| H | -0.88369900 | 3.95977300 | 0.73210400 |
| C | -5.75228600 | -1.26508900 | 0.37795200 |
| H | -5.63957400 | -2.03081100 | 1.15127200 |
| C | -6.84820800 | -1.31042800 | -0.48288700 |
| H | -7.58871200 | -2.10747100 | -0.37619400 |
| C | -4.94277600 | 0.70638000 | -0.74476400 |
| H | -4.20855000 | 1.50909200 | -0.84422700 |
| C | -6.99733200 | -0.34429300 | -1.47736500 |
| H | -7.85517700 | -0.37615400 | -2.15391300 |
| C | 2.60635300 | -2.34482400 | -3.33475100 |
| H | 1.64297600 | -2.80990600 | -3.59200700 |
| H | 3.37957300 | -2.82602400 | -3.95226800 |
| H | 2.55625400 | -1.29085600 | -3.64653200 |
| C | -6.04218600 | 0.66719000 | -1.59965900 |
| H | -6.15682000 | 1.43761400 | -2.36674000 |
| C | 0.85507800 | -4.72947000 | -1.41049200 |
| H | 1.44047400 | -4.73154000 | -2.33989700 |
| H | 0.05113000 | -5.47093500 | -1.53640400 |
| H | 1.50340900 | -5.09841000 | -0.60043600 |

**Table S12.** Optimized coordinates for $(SiP_2S)FeN_2$ with MeCN solvation (m06l, $S = 1$)

| Atom | Mulliken atomic spin density (e-) | Percentage of total spin density (%) |
|---|---|---|
| 1 Fe | 0.918617 | 57.54 |
| 2 P | 0.017703 | 1.11 |
| 3 S | 0.176109 | 11.03 |
| 4 P | 0.00877 | 0.55 |
| 5 Si | -0.086852 | 5.44 |
| 6 N | -0.007824 | 0.49 |
| 7 C | -0.004151 | 0.26 |
| 8 C | -0.004923 | 0.31 |
| 9 H | -0.000571 | 0.04 |
| 10 C | -0.003273 | 0.21 |
| 11 C | 0.039217 | 2.46 |
| 12 C | 0.002189 | 0.14 |
| 13 C | -0.021828 | 1.37 |
| 14 H | 0.000714 | 0.04 |
| 15 C | 0.008125 | 0.51 |
| 16 H | 0.00059 | 0.04 |
| 17 C | -0.000679 | 0.04 |
| 18 H | -0.000058 | 0 |
| 19 C | 0.00837 | 0.52 |
| 20 H | 0.002665 | 0.17 |
| 21 C | -0.000748 | 0.05 |
| 22 H | 0.000084 | 0.01 |
| 23 C | 0.042411 | 2.66 |
| 24 H | -0.002586 | 0.16 |
| 25 C | -0.004668 | 0.29 |
| 26 H | -0.000517 | 0.03 |
| 27 C | 0.003183 | 0.2 |
| 28 C | 0.000803 | 0.05 |
| 29 H | -0.000086 | 0.01 |
| 30 C | 0.000523 | 0.03 |
| 31 H | -0.000615 | 0.04 |
| 32 H | -0.000202 | 0.01 |
| 33 H | 0.000013 | 0 |
| 34 C | 0.047127 | 2.95 |
| 35 C | 0.00096 | 0.06 |
| 36 H | -0.000086 | 0.01 |
| 37 C | -0.000735 | 0.05 |
| 38 H | 0.000194 | 0.01 |
| 39 H | 0.000108 | 0.01 |
| 40 H | 0.001205 | 0.08 |
| 41 C | -0.00438 | 0.27 |
| 42 C | -0.03821 | 2.39 |
| 43 C | 0.000202 | 0.01 |

| | | |
|---|---|---|
| 44 H | 0.000416 | 0.03 |
| 45 H | -0.000009 | 0 |
| 46 H | 0.000274 | 0.02 |
| 47 C | -0.000714 | 0.04 |
| 48 H | -0.000067 | 0 |
| 49 C | -0.020507 | 1.28 |
| 50 H | 0.00072 | 0.05 |
| 51 C | 0.000177 | 0.01 |
| 52 H | 0.000025 | 0 |
| 53 H | 0.000139 | 0.01 |
| 54 H | 0.001091 | 0.07 |
| 55 C | -0.000763 | 0.05 |
| 56 H | 0.000027 | 0 |
| 57 C | 0.000792 | 0.05 |
| 58 H | -0.000076 | 0 |
| 59 C | -0.000393 | 0.02 |
| 60 H | -0.000019 | 0 |
| 61 H | -0.000194 | 0.01 |
| 62 H | 0.000553 | 0.03 |
| 63 N | -0.061058 | 3.82 |
| 64 C | 0.000775 | 0.05 |
| 65 H | -0.00012 | 0.01 |
| 66 C | 0.000773 | 0.05 |
| 67 H | 0.000602 | 0.04 |
| 68 H | 0.000277 | 0.02 |
| 69 H | -0.000104 | 0.01 |
| 70 C | 0.003106 | 0.19 |
| 71 H | -0.000147 | 0.01 |
| 72 C | -0.000981 | 0.06 |
| 73 H | 0.000074 | 0 |
| 74 C | 0.002351 | 0.15 |
| 75 H | 0.000382 | 0.02 |
| 76 C | 0.002736 | 0.17 |
| 77 H | -0.000133 | 0.01 |
| 78 C | 0.000223 | 0.01 |
| 79 H | 0.000135 | 0.01 |
| 80 H | 0.000069 | 0 |
| 81 H | 0.000715 | 0.04 |
| 82 C | -0.00105 | 0.07 |
| 83 H | 0.000133 | 0.01 |
| 84 C | 0.00053 | 0.03 |
| 85 H | -0.000059 | 0 |
| 86 H | 0.001241 | 0.08 |
| 87 H | 0.000052 | 0 |
| 88 H | -0.028886 | 1.81 |

**Table S13.** Mulliken atomic spin densities calculated for **8-H** (gas-phase, m06l, $S = 1/2$)


[1] McGinley, P. L.; Koh, J. T. *J. Am. Chem. Soc.* **2007**, *129*, 3822-3823.
[2] Takaoka, A.; Mankad, N. P.; Peters, J. C. *J. Am. Chem. Soc.* **2011**, *133*, 8440-8443.
[3] Bhattacharyya, K. X.; Dreyfuss, S.; Saffon-Merceron, N.; Mézailles, N. *Chem. Commun.* **2016**, *52*, 5179-5182.
[4] Gaussian 09, Revision B.01, M.J. Frisch, G. W. Trucks, H. B. Schlegel, G. E. Scuseria, M. A. Robb, J. R. Cheeseman, G. Scalmani, V. Barone, B. Mennucci, G. A. Petersson, H. Nakatsuji, M. Caricato, X. Li, H. P. Hratchian, A. F. Izmaylov, J. Bloino, G. Zheng, J. L. Sonnenberg, M. Hada, M. Ehara, K. Toyota, R. Fukuda, J. Hasegawa, M. Ishida, T. Nakajima, Y. Honda, O. Kitao, H. Nakai, T. Vreven, J. A. Montgomery Jr., J. E. Peralta, F. Ogliaro, M. Bearpark, J. J. Heyd, E. Brothers, K. N. Kudin, V. N. Staroverov, R. Kobayashi, J. Normand, K. Raghavachari, A. Rendell, J. C. Burant, S. S. Iyengar, J. Tomasi, M. Cossi, N. Rega, J. M. Millam, M. Klene, J. E. Knox, J. B. Cross, V. Bakken, C. Adamo, J. Jaramillo, R. Gomperts, R. E. Stratmann, O. Yazyev, A. J. Austin, R. Cammi, C. Pomelli, J. W. Ochterski, R. L. Martin, K. Morokuma, V. G. Zakrzewski, G. A. Voth, P. Salvador, J. J. Dannenberg, S. Dapprich, A. D. Daniels, Ö. Farkas, J. B. Foresman, J. V. Ortiz, J. Cioslowski, D. J. Fox, Gaussian, Inc., Wallingford CT, 2009.
[5] Zhao, Y.; Truhlar, D. G. *J. Chem, Phys.* **2006**, *125*, 194101.
[6] Weigend, F.; Ahlrichs, R. *Phys. Chem. Chem. Phys.* **2005**, *7*, 3297–3305.
[7] Warren, J. J.; Tronic, T. A.; Mayer, J. M. *Chem. Rev.* **2010**, *110*, 6961-7001.
[8] Stoll, S.; Schweiger, A. *J. Magn. Reson*. **2006**, *178*, 42-55.